

# Rate-Splitting Multiple Access: Unifying NOMA and SDMA in MISO VLC Channels

## (Invited Paper)

Shimaa Naser, Lina Bariah, *Member, IEEE*, Wael Jaafar, *Senior Member, IEEE*,  
Sami Muhaidat, *Senior Member, IEEE*, Paschalis C. Sofotasios, *Senior Member, IEEE*,  
Mahmoud Al-Qutayri, *Senior Member, IEEE*, and Octavia A. Dobre, *Fellow, IEEE*

The increased proliferation of connected devices requires a paradigm shift towards the development of innovative technologies for the next generation of wireless systems. One of the key challenges, however, is the spectrum scarcity, owing to the unprecedented broadband penetration rate in recent years. Visible light communications (VLC) has recently emerged as a possible solution to enable high-speed short-range communications. However, VLC systems suffer from several limitations, including the limited modulation bandwidth of light-emitting diodes. Consequently, several multiple access techniques (MA), e.g., space-division multiple access (SDMA) and non-orthogonal multiple access (NOMA), have been considered for VLC networks. Despite their promising multiplexing gains, their performance is somewhat limited. In this article, we first provide an overview of the key MA technologies used in VLC systems. Then, we introduce rate-splitting multiple access (RSMA), which was initially proposed for RF systems and discuss its potentials in VLC systems. Through system modeling and simulations of an RSMA-based two-use scenario, we illustrate the flexibility of RSMA in generalizing NOMA and SDMA, as well as its superiority in terms of weighted sum rate (WSR) in VLC. Finally, we discuss challenges, open issues, and research directions, which will enable the practical realization of RSMA in VLC.

**Index Terms**—Multiple-input multiple-output (MIMO), non-orthogonal multiple access (NOMA), space-division multiple access (SDMA), rate-splitting multiple access (RSMA), visible light communications (VLC).

### I. INTRODUCTION

THE exponential growth of connected devices and emergence of the Internet-of-Everything (IoE), enabling ubiquitous connectivity among billions of people and machines, have been the major driving forces towards the evolution of wireless technologies, aiming to support a plethora of new services, including enhanced mobile broadband and ultra-reliable and low-latency communications. While the demand for new IoE services, e.g., extended reality, autonomous driving and tactile Internet continues to grow, it is necessary for future wireless networks to deliver high reliability, low latency, and very high data rates. In this context, the notion of visible light communications (VLC) has emerged as a promising wireless technology for massive connectivity of users with high data rates.

To realize VLC, a simple and inexpensive modification is required to the existing lighting infrastructure [1]–[4]. The key attractive features of VLC include, but are not limited to, security, high degree of spatial reuse, and immunity to

electromagnetic interference [5]. The advancement in solid-state has introduced light emitting diodes (LEDs) as energy-efficient light sources, which are envisioned to dominate the next generation of wireless infrastructure. One of the interesting features of LEDs is their ability to rapidly switch between different light intensities in a way that is not perceptible to human eyes. This enables them to be the main technology for VLC systems. The key principle of VLC is to use emitted light from the LEDs to perform data transmission through intensity modulation and direct detection (IM/DD), without affecting the LEDs' main illumination function. The huge unregulated spectrum of visible light allows VLC to offload data traffic from radio-frequency (RF)/microwave systems while providing high data rates. VLC uses the 400 THz to 789 THz visible light spectrum, which is characterized by the features of low penetration through objects, secure communications, and high quality-of-service (QoS) in interference-free small cells designs [6]–[8]. Fig. 1 shows the VLC spectrum band and examples of its use in healthcare, work office, transportation, and smart cities. Also, the structure of the survey is illustrated in Fig. 2.

#### A. Motivation and Contribution

Despite its advantages, VLC suffers from several drawbacks that limit its performance. For example, the limited modulation bandwidth and peak optical power of LEDs are considered as the main obstacles towards realizing the full potential of VLC systems [9]. Therefore, several studies have been carried out to enhance the spectral efficiency of VLC systems. In particular, two research directions have been identified: in the first one, researchers focused on the design of dedicated VLC analog hardware and digital signal processing techniques. In

S. Naser, L. Bariah and S. Muhaidat are with the Center for Cyber-Physical Systems, Department of Electrical Engineering and Computer Science, Khalifa University, Abu Dhabi, UAE, (e-mails: 100049402@ku.ac.ae; lina.bariah@ku.ac.ae; muhaidat@ieee.org.)

P. C. Sofotasios is with the Center for Cyber-Physical Systems, Department of Electrical Engineering and Computer Science, Khalifa University, Abu Dhabi, UAE, and also with the Department of Electrical Engineering, Tampere University, Tampere, Finland, (e-mail: p.sofotasios@ieee.org.)

M. Al-Qutayri is with the Department of Electrical Engineering and Computer Science, Khalifa University, Abu Dhabi, UAE, (e-mail: mahmoud.alqutayri@ku.ac.ae.)

W. Jaafar is with the Department of Systems and Computer Engineering, Carleton University, Ottawa, ON, Canada, (e-mail: waeljaafar@sce.carleton.ca.)

O. A. Dobre is with the Faculty of Engineering and Applied Science University, Memorial University, St. John's, Canada, (e-mail: odobre@mun.ca.)

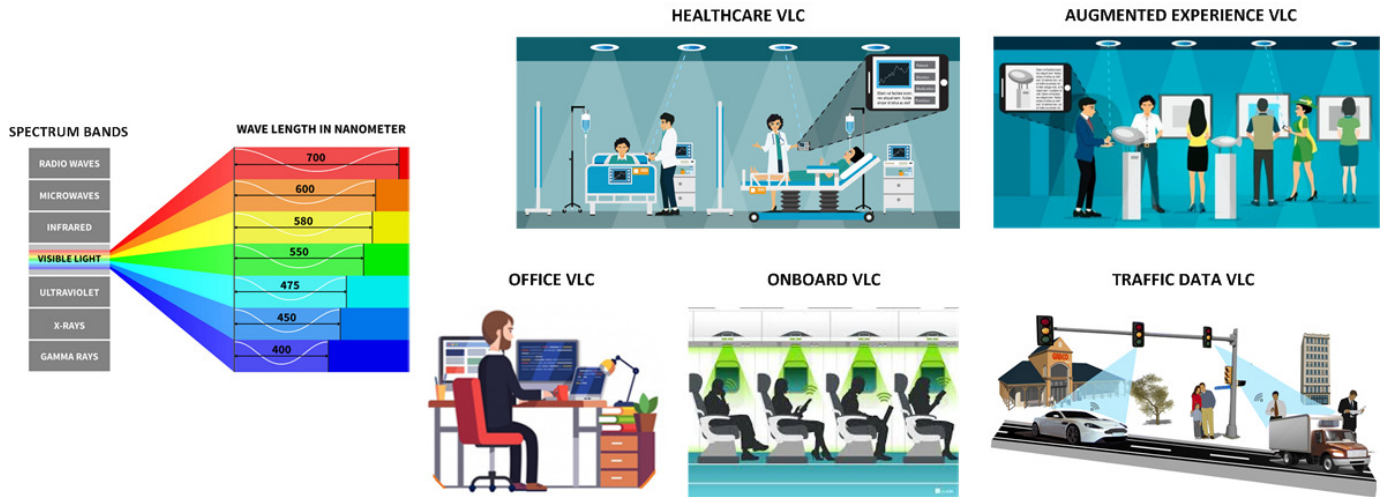


Fig. 1. VLC spectrum and examples of its use.

TABLE I  
LIST OF ACRONYMS AND ABBREVIATIONS.

Abbreviation	Definition	Abbreviation	Definition
ADT	Angle Diversity Transmitter	MU	Multi-User
AO	Alternating Optimization	MUD	Multi-User Detection
BD	Block Diagonalization	MUI	Multi-User Interference
BER	Bit Error Rate	NOMA	Non-Orthogonal Multiple Access
BC	Broadcast Channel	OCDMA	Optical Code-Division Multiple Access
CDMA	Code-Division Multiple Access	OFDM	Orthogonal Frequency-Division Multiplexing
C-NOMA	Code NOMA	OFDMA	Orthogonal Frequency-Division Multiple Access
CoMP	Coordinated multi-point	OMA	Orthogonal Multiple Access
CSI	Channel State Information	OOK	On-Off Keying
CSIT	CSI at Transmitter	P-NOMA	Power NOMA
DC	Direct Current	PD	Photo Detectors
DD	Direct Detection	QoS	Quality-of-Service
FoV	Field of View	RGB	Red, Green and Blue
ICI	Inter-Channel Interference	RSMA	Rate-splitting Multiple Access
IM	Intensity Modulation	SC	Super-position Coding
ISI	Inter-Symbol Interference	SDMA	Space Division Multiple Access
LED	Light Emitting Diode	SIC	Successive Interference Cancellation
LTE	Long-Term Evolution	SINR	Signal-to-Interference-Plus-Noise Ratio
LoS	Line-of-Sight	SNR	Signal-to-Noise Ratio
MA	Multiple Access	TDMA	Time-Division Multiple Access
MAC	Media Access Control	VLC	Visible Light Communication
MIMO	Multiple-Input Multiple-Output	WSMSE	Weighted Sum Mean Squared Error
MISO	Multiple-Input Single-Output	WSR	Weighted Sum Rate
MMSE	Minimum Mean-Square Error	ZF	Zero-Forcing
MSE	Mean-Square Error	ZF-DPC	Zero-Forcing Dirty-Paper

the second one, researchers focused on enhancing the spectral efficiency through the development of different optical-based modulation and coding schemes, adaptive modulation, equalization, VLC cooperative communications, orthogonal and non-orthogonal multiple access (OMA/NOMA) schemes, and multiple-input multiple-output (MIMO) [10].

In the context of VLC, several optical OMA schemes have been proposed, including time-division multiple access (TDMA), orthogonal frequency-division multiple access (OFDMA) [11], and optical code-division multiple access (OCDMA) [12]. These schemes rely on assigning orthogonal resources to different users. For example, in TDMA, different users are allocated different time slots for communication, while in OFDMA different users are assigned different orthogonal frequency sub-carriers. In OCDMA, users communicate at the same time and frequency, which can be achieved through the use of different orthogonal optical codes.

In contrast, space-division multiple access (SDMA) exploits the spatial separation between users to provide full time and frequency resources. On the contrary, NOMA has been recently introduced as a spectrum-efficient multiple access (MA) scheme that allows different users to share the same time and frequency resources, leading to an enhanced spectral efficiency [13]. NOMA is realized either by assigning different power levels to different users (known as power (P)-NOMA) or by allocating different spreading sequences (called code (C)-NOMA). Resource allocation in NOMA is determined according to different criteria, such as link quality, users fairness, targeted individual and sum rates, and users' QoS requirements.

In the same context, rate-splitting multiple access (RSMA) has recently emerged as a potentially robust and generalized MA scheme for future wireless systems, which is able to accommodate different users in a heterogeneous environment.

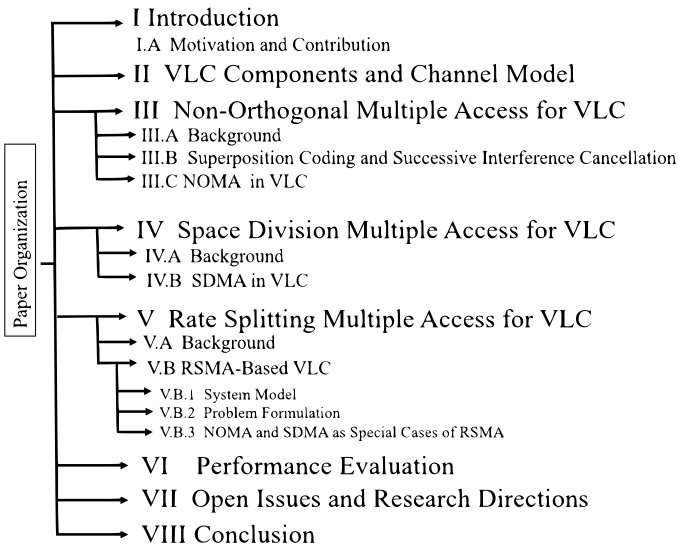


Fig. 2. Organization of the paper.

In particular, novel research results have shown that RSMA in MIMO-based RF systems outperforms other common MA schemes, such as NOMA and SDMA, in terms of spectral efficiency [14]. The performance gain of RSMA comes from the fact that the transmitted signal of each user is divided into one or several common parts and a private part. All common parts are multiplexed and encoded into a single (or several) common streams intended for all (or to a subset of) users. On the other hand, the private parts are encoded separately into multiple private streams, which are then superimposed with the common stream(s). The super-symbol is then transmitted to all users over the VLC downlink. At each user, the common streams are decoded first in order to obtain the common parts of the intended user, utilizing iterative successive interference cancellation (SIC). Subsequently, the private part is decoded while treating the other users' private parts as noise. The NOMA scheme can be obtained from RSMA by treating some users' signals as common parts and the remaining as private parts. On the other hand, SDMA can be realized from RSMA by using only the private parts to encode users' messages. The split of the messages into common and private parts enables RSMA to provide robust services for different network loads and users deployments.

In VLC systems, MIMO channels are practically highly correlated, which inevitably degrades the performance of linear precoding schemes. This has motivated the investigation of different receiver structures and precoding schemes in order to mitigate the effect of channel correlation in MIMO VLC systems. Likewise, several articles on the previously presented topics, namely OMA, NOMA and RSMA techniques design, have been presented for RF systems. Yet, only few have addressed their application in VLC networks (mainly for OMA and NOMA), and summarized these studies in surveys [15]–[17]. Moreover, none of them has discussed the integration of RSMA into VLC systems. Motivated by the above, in this survey, we shed the light on several spectrally efficient MA schemes for VLC systems. In more details, we present

a comprehensive study of NOMA and SDMA schemes, with particular attention to MIMO-VLC systems. In addition, we address the potential integration of the RSMA scheme in MIMO-VLC systems. Finally, open issues and some interesting related research directions are discussed.

*Notation:* Bold upper-case letters denote matrices and bold lower-case letters denote vectors.  $(\cdot)^T$  denotes the transpose operation,  $\mathbb{E}(\cdot)$  is the statistical expectation operation,  $|\cdot|$  is the absolute value operation,  $\mathbf{I}$  is the identity matrix,  $\mathbf{0}$  is the zero matrix,  $\text{tr}(\cdot)$  is the trace of a matrix, and  $\mathcal{N}(0, \sigma^2)$  is a real-value Gaussian distribution with zero mean and variance  $\sigma^2$ . Let  $\mathbf{z} = [z_1, \dots, z_Z]$  be a vector of length  $Z$ , then  $L_1(\mathbf{z}) = \sum_{i=1}^Z |z_i|$  is the  $L_1$  norm.

## II. VLC COMPONENTS AND CHANNEL MODEL

In VLC, unlike RF systems, data is conveyed on the intensity of the emitted light from the LEDs, therefore, frequency and phase modulations cannot be applied. Moreover, due to the characteristics of intensity modulation, transmitted signals must be positive and real valued. Also, to ensure that the LED is functioning in its dynamic range, the transmitted peak power should not exceed a particular constant value. In this section, different components of VLC systems are presented in addition to VLC channel modeling.

Fig. 3 illustrates the basic VLC transceiver components. At the transmitter, an illuminating device is utilized for data modulation through IM/DD. There are a variety of light sources that are available for optical communication, but the commonly used ones are LEDs and laser diodes. Particularly, LEDs are the most popular illuminating devices, due to their low fabrication cost. They are composed of solid-state semiconductor devices that produce spontaneous optical radiation when subjected to a voltage bias across the P-N junction [18]. The direct current (DC) bias excites the electrons resulting in released energy in the form of photons. In most buildings, white LEDs are preferred since objects seen under white LEDs have similar colors to when seen under natural light. Two common designs are considered for white LEDs. In the first design, a blue LED with a yellow phosphor layer is utilized, while in the second design, red, green, and blue (RGB) LEDs are combined together. The first method is more popular, due to its simplicity and low implementation cost. However, it suffers from limited modulation bandwidth due to the intrinsic properties of the phosphor coating. On the other hand, RGB LEDs are more suitable for color shift keying modulation, enabling higher achievable data rates [19].

It is recalled that VLC receivers comprise photo detectors (PDs), also known as non-imaging receivers or imaging (camera) sensors. These are used in order to convert incident light power into electrical current proportional to light intensity. A typical VLC receiver consists of an optical filter, optical concentrator, PDs and pre-amplifier. The optical filter eliminates interference from ambient light sources, while the optical concentrator enlarges the effective reception area of the PD without increasing its physical size. The optical concentrator is characterized by three parameters, i.e., field of view (FoV), refractive index, and radius. In order to increase

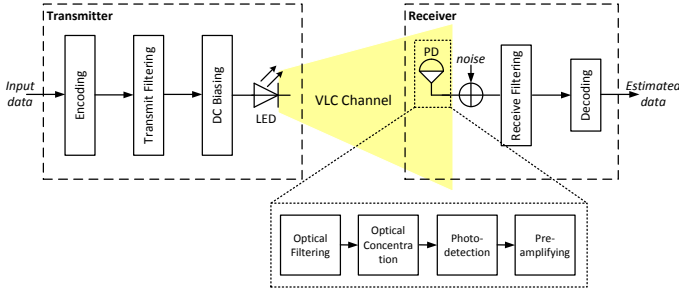


Fig. 3. VLC transceiver components.

the achievable diversity gain of an optical communication link, multiple receiving units can be deployed with different orientations, optical filters, and concentrators. However, such deployment comes at the expense of additional receiver size and complexity. To address this issue, an imaging sensor with a single wide FoV concentrator can be used to create multiple images of the received signals. Imaging sensors consist of an array of PDs that are integrated with the same circuit. It is worth noting that the required large number of PDs to capture high resolution photos renders them energy inefficient. It is noted that the PDs area of a VLC system is much larger than the corresponding wavelength. Consequently, the multipath fading in an indoor VLC environment does not occur [20], [21]. Nevertheless, indoor optical links suffer from dispersion, modeled as linear baseband impulse response. Also, the indoor optical wireless channels can be assumed quasi-static, due to the relatively low mobility of users and connected objects in indoor environments.

Typically, the channel of a VLC link can be modeled as follows: With the non-line-of-sight components neglected in front of stronger line-of-sight (LoS) ones, the DC channel gain from the  $i^{\text{th}}$  LED to the  $k^{\text{th}}$  PD can be expressed by [1]

$$h_{k,i} = \begin{cases} \frac{A_k}{d_{k,i}^2} R_o(\varphi_{k,i}) T_s(\phi_{k,i}) g(\phi_{k,i}) \cos(\phi_{k,i}), & 0 \leq \phi_{k,i} \leq \phi_c \\ 0, & \text{otherwise,} \end{cases} \quad (1)$$

where  $A_k$  denotes the PD area,  $d_{k,i}$  is the distance between the  $i^{\text{th}}$  LED and  $k^{\text{th}}$  PD,  $\varphi_{k,i}$  is the transmission angle from the  $i^{\text{th}}$  LED to the  $k^{\text{th}}$  PD,  $\phi_{k,i}$  denotes the incident angle with respect to the receiver, and  $\phi_c$  is the FoV of the PD. These angles are well-illustrated in Fig. 4. Moreover,  $T_s(\phi_{k,i})$  is the gain of the optical filter, and  $g(\phi_{k,i})$  is the gain of the optical concentrator, expressed as

$$g(\phi_{k,i}) = \begin{cases} \frac{n^2}{\sin^2(\phi_c)}, & 0 \leq \phi_{k,i} \leq \phi_c \\ 0, & \phi_{k,i} > \phi_c. \end{cases} \quad (2)$$

Here,  $n$  is the refractive index and  $R_o(\varphi_{k,i})$  is the Lambertian radiant intensity given by

$$R_o(\varphi_{k,i}) = \frac{m+1}{2\pi} (\cos(\varphi_{k,i}))^m \quad (3)$$

with  $m$  denoting the order of the Lambertian emission, namely

$$m = \frac{\ln(2)}{\ln(\cos(\varphi_{1/2}))} \quad (4)$$

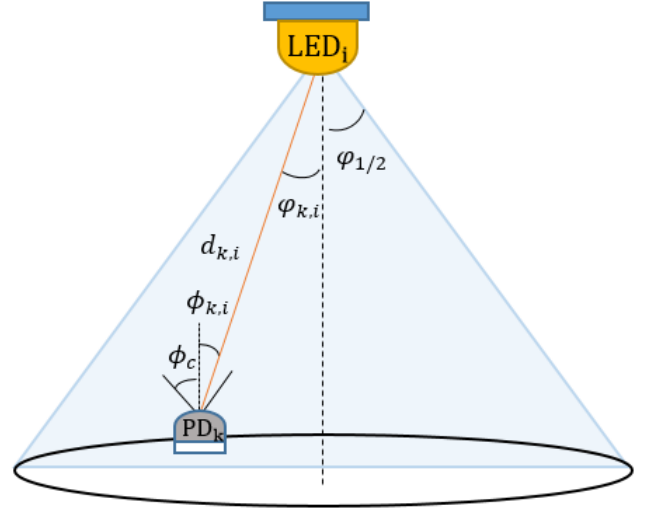


Fig. 4. VLC channel model (link between LED  $i$  and PD  $k$ ).

where  $\varphi_{1/2}$  is the LED semi-angle at half power. For a typical VLC link, the received noise at the  $k^{\text{th}}$  PD can be modeled as a Gaussian random variable with zero mean and variance

$$\sigma_k^2 = \sigma_{k,\text{sh}}^2 + \sigma_{k,\text{th}}^2 \quad (5)$$

where  $\sigma_{k,\text{sh}}^2$  and  $\sigma_{k,\text{th}}^2$  are the variances of the shot and thermal noises at the  $k^{\text{th}}$  PD, respectively. The shot noise is caused by the high rate of the physical photo-electronic conversion process, whose variance can be written as

$$\sigma_{k,\text{sh}}^2 = 2qB(\zeta_k h_{k,i} x_i + I_{\text{bg}} I_2) \quad (6)$$

where  $q$  represents the electronic charge, while  $\zeta_k$  denotes the detector responsivity. Also,  $x_i$  is the transmitted signal by the  $i^{\text{th}}$  LED,  $B$  is the corresponding bandwidth,  $I_{\text{bg}}$  is the background current, and  $I_2$  denotes the noise bandwidth factor. On the other hand, the thermal noise results from the transimpedance receiver circuitry and its variance at the  $k^{\text{th}}$  PD is given by

$$\sigma_{k,\text{th}}^2 = \frac{8\pi K T_k}{G} \eta A_k I_2 B^2 + \frac{16\pi^2 K T_k \gamma}{g_m} \eta^2 A_k^2 I_3 B^3 \quad (7)$$

where  $K$  is the Boltzmann's constant,  $T_k$  is the absolute temperature,  $G$  is the open-loop voltage gain,  $A_k$  is the PD area,  $\eta$  is the PD's fixed capacitance per unit area,  $\gamma$  is the field-effect transistor (FET) channel noise factor,  $g$  is the FET transconductance, and  $I_3 = 0.0868$  [1]. Modern infrastructures are commonly equipped with LED fixtures or arrays. A single fixture is composed of  $Q$  LEDs, and may be viewed as a single VLC source,<sup>1</sup> with the DC channel gain given by

$$h_{k,j} = \begin{cases} A_k \sum_{i=1}^Q d_{k,j,i}^{-2} R_o(\varphi_{k,j,i}) T_s(\phi_{k,j,i}) g(\phi_{k,j,i}) \cos(\phi_{k,j,i}), & 0 \leq \phi_{k,j,i} \leq \phi_c \\ 0, & \text{otherwise} \end{cases} \quad (8)$$

<sup>1</sup>In the remaining of this paper, we interchangeably designate by LED a fixture of LEDs.

where  $d_{k,j,i}$  and  $\varphi_{k,j,i}$  denote the respective distance and transmission angle between the  $i^{\text{th}}$  LED in the  $j^{\text{th}}$  fixture and the  $k^{\text{th}}$  PD, and  $\phi_{k,j,i}$  is the incident angle with respect to the receiver. Since the separation between LEDs in the same fixture is negligible compared to the distance between the fixture and the  $k^{\text{th}}$  PD, then distances and angles implicating index  $i$  can be assumed approximately the same for all LEDs. Hence, the channel gain from the  $j^{\text{th}}$  fixture to the  $k^{\text{th}}$  PD can be given by

$$h_{k,j} \approx \begin{cases} Q h_{k,i}, & 0 \leq \phi_{k,j,i} \leq \phi_c, \forall i \\ 0, & \text{otherwise.} \end{cases} \quad (9)$$

In the following sections, we provide an in-depth study of the common MA schemes in the context of VLC.

### III. NOMA FOR VLC

#### A. Background

Inspired by promising multiplexing gains achieved by conventional MA techniques, which were developed for RF systems, optical MA have received great attention recently. To this end, conventional OMA schemes such as OFDMA and TDMA have been extensively studied in the context of VLC, in which users are allocated orthogonal frequency/time resources. In the same context, several optical OFDM-based MA techniques were proposed, such as DC biased optical OFDM, asymmetrically clipped OFDM, asymmetrically clipped DC-biased optical OFDM, fast-OFDM and, polar-OFDM. However, OFDM suffers from high peak-to-average power ratio, which is difficult to overcome in VLC systems due to the non-linearity of LEDs [11], [22]–[25]. OMA schemes efficiently mitigate interference among users' signals by allocating orthogonal resources. However, the number of served users is limited and cannot exceed the number of available orthogonal resources. This concern is also true for VLC systems.

Motivated by the above, researchers have recently focused on the design of novel NOMA techniques as a promising candidate to enhance spectral efficiency in 5G and beyond networks [13]. The key principle is to allow different users to share the same frequency resources simultaneously at the expense of multi-user interference (MUI). To perform multi-user detection (MUD), different users are assigned distinct power levels based on their channels gain, which is referred to as P-NOMA, or different spreading sequence, known as C-NOMA [13], [26], [27]. In RF systems, P-NOMA was considered as a candidate for the downlink communication of various standardizations activities such as the 3rd generation partnership project (3GPP) standard LTE Release 13 [28]. Furthermore, P-NOMA has been envisioned as a key solution in 5G mobile systems [20]. On the other hand, both P-NOMA and C-NOMA have been considered for the uplink communication, in order to serve a larger number of users. In downlink P-NOMA systems, superposition coding (SC) at the base station and SIC at the receiver are utilized to transmit and detect the intended user's signal by eliminating users' signals with higher power levels, respectively. While, in the uplink P-NOMA systems, the transmitted power is limited by the end users, the transmitted power of each individual user should be

carefully adjusted such that the user with better channel gain will have more power contribution in the received signal. At the base station, the user with the best channel gain is decoded first. Then, a subsequent SIC is performed in order to decode the messages of the weaker users, which is the opposite of the downlink P-NOMA [20], [28].

In C-NOMA, users are multiplexed in the code domain, in which each user is assigned a different code. Unlike the conventional code-division multiple access (CDMA), where dense spreading sequences are used, C-NOMA utilizes non-orthogonal sequences with low cross correlation or sparse spreading sequences to efficiently reduce the inter-user interference [29]–[32], and hence, enhance the overall system performance. Specifically, optimal performance can be achieved in C-NOMA based VLC systems by exploiting optical code sequences [33]. At the receiver, multi-user detection can then be realized by adopting message passing algorithms (MPA). It is noted that different versions of C-NOMA have been developed, such as low-density spreading (LDS)-CDMA [34], low-density spreading (LDS)-OFDM [35], and sparse code multiple access (SCMA) [36]. LDS-CDMA utilizes low density spreading sequences in order to reduce the interference on each chip compared to the traditional CDMA. On the other hand, LDS-OFDM can be thought as a combination of both OFDM and LDS-CDMA, where the resulted chips from the implementation of LDS-CDMA are transmitted over a set of sub-carriers. Finally, SCMA is a form of LDS-CDMA, where the information bits can be directly mapped to a distinct sparse codeword. Yet, although C-NOMA has a potential to enhance spectral efficiency, it requires additional bandwidth, challenging codebook design and is not easily applicable to the current systems compared to P-NOMA, which has a simple implementation in the existing networks. For these reasons, most of the research on NOMA systems have extensively considered the performance of P-NOMA [20], [37], [38]. In VLC systems, the research on C-NOMA is limited only to [32]. Therefore, it requires further investigation in the context of VLC. It is also worth noting that uplink VLC is impractical due to the power limitations of portable devices and the unpleasant radiance produced by end users. So, it is expected that the current VLC technologies will rely on RF or infrared in the uplink communications [39]–[41]. Consequently, most of the research efforts on NOMA in VLC systems have focused on the downlink scenario. A basic system model for two-user downlink P-NOMA in VLC systems is illustrated in Fig. 5.

For indoor VLC systems, P-NOMA is preferred for several reasons [42]. First, P-NOMA depends on the channel state information, which can be readily available in VLC systems. Second, P-NOMA achieves the best performance in the high SNR regime, which is a common SNR regime in VLC channels [3]. Third, P-NOMA performs best when users' channels are distinct. In VLC systems, the underlying symmetry issue of the channels has been addressed in [43], where the authors proposed reducing channels' symmetry by an adaptive tuning of the semi-angle of the LEDs and the receiver's FoV, as well as in [44], where advance receiver structures were considered. Finally, P-NOMA can be easily integrated with

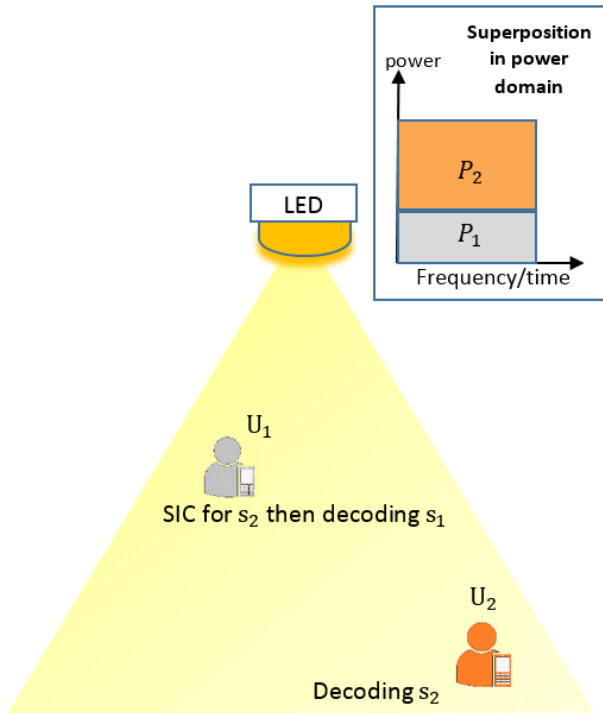


Fig. 5. Scenario of two users P-NOMA in VLC.

various technologies, such as MIMO and cooperative networks [36]. All these reasons motivated an important study focus on P-NOMA based VLC systems.

### B. Superposition Coding and Successive Interference Cancellation

SC was first introduced in 1972 by Cover [45] as a method to transmit different signals to several receivers through a single source. To make SC practical, the transmitter encodes the data of two users as a two-layer single signal. Then, one receiver recovers the messages of the two layers, while the other recovers only one message from one-layer and ignores the message of the second layer. SC is realized by allocating higher power coefficients to users with the weakest channel conditions. On the other hand, users with strongest channel gains are assigned the lowest power levels [28]. For instance, in Fig. 5, the second user  $U_2$  is allocated fraction  $P_2$  of the total power, and the first user  $U_1$  is allocated  $P_1$ , such that  $P_1 < P_2$ . Since the weaker user  $U_2$  is allocated higher power, it can directly decode its signal while treating the signals of the other users as noise. On the other hand, using SIC,  $U_1$  has to remove the interference by decoding  $U_2$  signal, before detecting its own signal.

### C. NOMA in VLC

Several studies have considered the performance of different NOMA configurations in VLC systems. In [31], the symbol error rate (SER) of C-NOMA-based VLC system was investigated, where users demonstrated identical error rate

performance at different locations. On the other hand, recent published papers have shown that in VLC systems, P-NOMA is an efficient MA scheme for the aforementioned reasons [43], [46], [47]. Furthermore, reported results showed that NOMA<sup>2</sup> outperforms OMA techniques, such as OFDMA and TDMA, in terms of system capacity and number of simultaneously served users, particularly in single-input single-output broadcast channels and for certain channel strength disparities among users [48]–[51]. The work in [52] considered the performance of NOMA VLC system when users have random vertical orientations. In particular, the authors proposed users scheduling techniques and feedback mechanisms to boost the spectral efficiency. Moreover, a hybrid NOMA-OFDM system was investigated and shown to have superior performance in terms of the achievable rate over OMA-OFDM systems [53], [54]. Likewise, for uplink NOMA-based VLC communications, joint detection was proposed in [55] to decode the messages of multiple users.

Although NOMA is efficient for scenarios where the number of users is higher than the number of available orthogonal resources, its complexity grows rapidly and proportionally to the number of users, since the  $k^{\text{th}}$  user needs to decode the messages of the  $k - 1$  users before detecting its own signal. To address this issue, a simple approach is to group users into small clusters, such that users of the same cluster communicate using NOMA, while the different clusters are scheduled using an OMA technique.

Particularly, MIMO can be leveraged to provide additional gains for transmissions, which can be realized through precoded SC and hybrid SDMA-NOMA or OMA. In precoded SC, all users are sorted based on their effective precoded channel gains in a single cluster [56]–[58]. On the contrary, in hybrid SDMA/NOMA/OMA, users are grouped in clusters separated by SDMA<sup>3</sup> [59], where the users of a single cluster are served using NOMA. It was demonstrated in [59] and [60] that MIMO-NOMA outperforms MIMO-OMA in terms of sum rate and user fairness. However, despite the aforementioned advantages of MIMO-NOMA systems, they come at the expense of a complex transmitter design, where joint optimization of signals precoding/decoding orders is required for different users.

As explained earlier, MIMO design can be realized by assuming multiple transmitting LEDs and multiple PDs at the receiver. Such a system cannot employ the same power allocation method designed for single transmitting LED NOMA VLC systems, such as gain ratio power allocation (GRPA) [21]. Accordingly, several power allocation strategies have been proposed in the literature for MIMO-NOMA RF systems, e.g., hybrid precoding and post-detection [61], and signal alignment [62], [63]. However, their counterpart in the MIMO-NOMA VLC is almost non-existent. To our knowledge, only Chen *et al.* investigated NOMA-based MIMO VLC systems and proposed a power allocation strategy, called normalized gain difference power allocation (NGDPA) [64]. The reported results for NGDPA illustrated a sum rate improvement of

<sup>2</sup>In the remaining of the paper, P-NOMA is designated by NOMA.

<sup>3</sup>SDMA is discussed in detail in Section IV.

29.1% compared to GRPA.

Multi-cell NOMA in the context of VLC has also not been well-investigated in the literature. In [65], Zhang *et al.* proposed a user grouping scheme based on users locations to minimize the interference caused by multi-cell deployment. Further, the authors in [66] proposed a joint NOMA transmission scheme to serve users in overlapping regions of different cells. In [67], Shi *et al.* investigated the use of offset quadrature amplitude modulation (OQAM)/OFDM-NOMA modulation in a multi-cell VLC system. Although NOMA schemes outperform OMA-based VLC systems in terms of spectral efficiency, the multiplexing gain of NOMA is highly affected by channel symmetry. In the context of VLC, channel symmetry is a major challenge as the communication is usually due to the LoS scenario [39], [42]. Indeed for small cell design, where the number of users is considered relatively large, it is inefficient to multiplex all users using NOMA, as this may lead to an increased complexity and unsuccessful SIC operation. Therefore, hybrid NOMA/OMA schemes are promising solutions to realize a trade-off between multiplexing gain, computational complexity, and error propagation. In hybrid NOMA/OMA systems, users are split into multiple groups, where users within the same group employ NOMA, while different groups are multiplexed using OMA. User pairing and grouping represents key challenge in hybrid NOMA/OMA systems that requires sophisticated algorithms to have the full potentials of NOMA. However in VLC systems, as users mobility is low, the variation in the channel conditions is relatively small, hence, user pairing and grouping requires less complicated algorithms compared to RF systems. The effect of user pairing and grouping has been extensively studied in RF systems [68]–[72], but, its application in VLC systems requires further investigations. For instance, in [49], [73], the authors adopted channel gain-based pairing strategy that aims to maximize the system's throughput. This strategy relies on selecting two users with the most distinctive channel gains to perform NOMA. However, their approach causes high interference to users with correlated channels. In [74], the authors proposed individual and group-based NOMA users pairing in a VLC system and showed that near-optimal sum-rate performance can be achieved. Moreover, user grouping based on users' locations was proposed in [65] in order to reduce the interference in VLC multi-cell networks, where users in each group are served by only one access point using NOMA. On the other hand, the authors in [75] proposed a hybrid OMA/NOMA scheme for attocellular VLC based on a smart transmitter to select dynamically the adequate MA technique according to the environment conditions. Finally, in [76], the authors proposed an efficient user pairing for the cases of having odd and even number of users. First users are ordered in ascending order based on the channel strength, then, they are either grouped into two or three groups depending on whether the number of the users is even or odd. Then pairing is performed by choosing one user from each group starting from the users with the lowest channel gain. Reducing channels' correlation for the end users is another method of enhancing the performance of NOMA system. In [43], the authors proposed an adaptive adjustment of the

semi-angle of the LEDs and the FoV of the PD in order to create dissimilar channels. Additionally, the use of different advanced receiver structures to reduce channels correlation is a potential solution that may be further investigated [44]. Nevertheless, the enhancement of NOMA performance through reducing channels symmetry need to be further explored in the context of VLC. Finally, it is noted that NOMA based hybrid VLC/RF systems have been proposed as acceptable solutions that compensate for the limitation of VLC systems, particularly in uplink communication scenarios [77]–[79]. In the same context, hybrid wavelength division multiplexing (WDM)-NOMA has been proposed in [80], where multi-color LEDs are used to allow simultaneous transmissions at different wavelengths. Relevant work on NOMA in VLC is summarized in Table II.

## IV. SDMA FOR VLC

### A. Background

In recent building designs, it is common to have multiple illuminating LEDs in indoor spaces. In VLC systems, channel access can be realized either through multiple access channel (MAC) or broadcast channel (BC). Most research effort has focused on the analysis of downlink BC of MU-MIMO, with an emphasis on the data rate performance. Such systems experience interference when orthogonal frequency/time resources are limited. MUI is a common issue in MU-MIMO systems, which can be eliminated at the receiver using an efficient MUD technique [81], [82]. However, the implementation of MUD in VLC systems suffers from high complexity and energy inefficiency. Therefore, SDMA, which is based on data precoding at the transmitter, constitutes a promising alternative solution.

### B. SDMA in VLC

An early implementation of SDMA is based on block diagonalization (BD), a generalized form of channel inversion precoding [83]. Although BD is a simple linear precoding technique, its application is limited to the scenario where the number of transmitting LEDs is larger than the total number of served users, i.e., overloaded regime. The authors in [84] used BD precoding in downlink MU-MIMO VLC and showed that BD is constrained by the correlation of the involved wireless links. Hence, a scheme that reduces this correlation was proposed, based on the adjustment of PDs' FoVs. Yu *et al.* developed in [85] linear zero-forcing (ZF) and ZF dirty paper coding (ZF-DPC) schemes in order to eliminate MUI and maximize the throughput or max-min fairness. However, in [86], the authors relaxed the ZF condition by applying the minimum mean squared error (MMSE) as a performance metric for the precoder design, in both perfect and imperfect CSI scenarios. In [87], an optimal mean squared error (MSE) precoder was designed in order to minimize the BER, under per-LED power constraints. The transceiver design was later simplified by adopting a ZF precoder. The corresponding results showed that the simplified scheme outperforms the conventional ZF precoder in terms of BER, while MSE achieves the best performance. Similar designs were proposed in [88], where an

TABLE II  
VLC RELATED WORK ON NOMA.

Reference	System Model	Objective	Findings
[31]	Single-cell downlink C-NOMA	Analysis and evaluation of the SER	Using adequate power allocation, users at different locations achieve almost an identical SER
[43]	Single-cell downlink NOMA	Derivation of closed-form expression for the bit error rate (BER)	Closed-form expressions match simulation results
[49]	Single-cell downlink NOMA	Derivation of closed-form expressions for the coverage probability and ergodic sum rate	NOMA outperforms conventional OMA scheme
[52]	Single-cell downlink NOMA	Derivation of closed-form expressions for the sum rate and outage probability	Analytical results agree with simulation results and near-optimal sum rate is achieved using a limited feedback scheme
[53], [54]	Single-cell downlink NOMA-OFDM	Maximization of the sum rate	NOMA-OFDM is superior to OMA-OFDM system, in terms of achievable data rate
[55]	Single-cell uplink NOMA	Evaluation of BER based on phase pre-distorted joint detection	Improved BER performance compared to NOMA based on SIC for different power values
[64]	MIMO-NOMA	Maximization of the sum rate	NGDPA improves the sum rate performance compared to GRPA
[65]	Downlink MU-multi-cell NOMA	Maximization of the sum rate and max-min rate criterion	User grouping and power allocation optimized, hence achieving higher sum user rate than OMA
[66]	Downlink MU-multi-cell NOMA	Maximization of the sum rate	Joint transmission (JT) NOMA achieves higher sum rates compared to the frequency reuse factor-2 NOMA
[67]	Downlink MU-multi-cell OQAM/OFDM-NOMA	Evaluation of spectral efficiency, BER, and error vector magnitude	Proposed scheme outperforms OFDM-NOMA and is more robust to inter-cell interference
[75]	Multi-cell hybrid OMA/NOMA	Evaluation of sum rate, outage probability, and fairness performances	Dynamically selecting the adequate MA technique achieves better performances than static configuration
[77], [78]	Downlink hybrid VLC/RF	Maximization of the sum rate	Optimal joint user grouping and power allocation based on game theory was proposed; this outperforms the standard opportunistic scheme
[79]	Cooperative NOMA VLC/RF with simultaneous wireless information and power transfer (SWIPT)	Derivation of closed-form expression for the outage probability	A trade-off on rate splitting allows outage performance balancing among users
[80]	Hybrid WDM-NOMA	Maximization of the sum rate	WDM-NOMA outperforms NOMA in terms of sum rate

optimal ZF precoder was obtained using an iterative concave-convex procedure, aiming at maximizing the achievable per-user data rate. Then, the authors simplified the precoder design using the high signal-to-noise ratio (SNR) approximation. In [89], Shen *et al.* proposed a different beamforming technique aiming at maximizing the sum rate of a virtual MIMO VLC system. Beamforming was designed using the sequential parametric convex approximation method, and it has been shown through simulations that it outperforms conventional ZF-based beamforming, particularly for highly correlated VLC channels and low optical transmit power. Likewise, Marshoud *et al.* developed in [90] an optical adaptive precoding for downlink MIMO VLC systems, under perfect and imperfect CSI. BER results showed that their scheme is more robust to imperfect CSI and channel correlation than conventional channel inversion precoding. Authors of [91] proposed precoding for an OFDM-based MU-MIMO VLC system, where precoding is applied at each sub-carrier, using ZF and MMSE techniques. This led to the enhancement of the sum rate performance at high SNR and for the case of uncorrelated channels. In [92], the sum rate maximization problem was reformulated as a weighted MMSE (WMMSE) problem to jointly design the BD precoding and receive filter coefficients. A similar approach was also considered in [93]. Finally, Adasme *et al.* proposed in [94] a hybrid approach, called spatial TDMA (STDMA),

where full connectivity is achieved by allowing simultaneous data rate transmission of multiple nodes within an optimized schedule.

The contribution in [95], [96] focused on precoding designs for coordinated multi-point (CoMP) MU-MIMO VLC systems. Through numerical analysis, the authors showed improvements in terms of signal-to-interference-plus-noise ratio (SINR) and weighted sum MSE (WSMSE), respectively. Additionally, Yin *et al.* considered in [97], [98] different SDMA grouping algorithms to obtain a trade-off between the Jain's fairness index and area spectral efficiency for a CoMP-VLC system through the utilization of linear ZF precoding. The authors in [99] proposed a joint precoder and equalizer design based on interference alignment for MU multi-cell MIMO VLC systems under imperfect CSI. In [100], different levels of coordination/cooperation were considered using a ZF precoder.

It is worth noting that SDMA can be also realized using an angle diversity transmitter (ADT), which consists of multiple directional narrow-beam LED elements. An ADT creates independent narrow-band beams (by reducing the FoVs of LEDs) towards spatially deployed users, while achieving the same coverage as a single wide-beam transmitter [101]–[103]. ADTs can also replace conventional single-element transmitters in multi-cell scenarios such that more power is directed towards



each user, and hence, improving the communication's reliability [104]. In order to avoid interference among users, spatial separation needs to be implemented by adequately allocating transmit power to the beams. Subsequently, each receiver attempts to detect its signal by treating any interference as noise. In spite of the ADT's interference reduction potential, it requires a complex optical front-end to supply independent signals to multiple LED elements.

Compared to NOMA, SDMA simplifies the transmitter and receiver designs. However, it becomes inefficient as soon as the number of users exceeds the number of transmit LEDs, i.e., an overloaded scenario. It should be noted that the number of LEDs has to be more than or equal to the number of users in order to guarantee interference reduction. Moreover, since SDMA depends highly on the CSI at the transmitter (CSIT) in order to mitigate interference, its performance degrades with imperfect CSI [90], [105], [106]. Finally, due to the unique characteristics of IM/DD, which require signals to be real and unipolar, it is very difficult to pair orthogonal users together, as in RF systems. The accomplished work on SDMA in VLC is summarized in Table III.

## V. RSMA FOR VLC

Although NOMA realizes simultaneous transmission of a large number of users in overloaded scenarios and SDMA achieves spatial separation between users in underloaded scenarios, their performance is highly dependent on users' deployments, channel conditions, and availability of CSIT. Therefore, a generalized configuration, which can optimize the utilization of resources for both overloaded and underloaded scenarios and provide more robustness to CSIT estimation errors, is of paramount importance. This was the main motivation behind the proposal of RSMA as a generalized scheme, where NOMA and SDMA can be considered as special cases.

### A. Background

The basic concept of rate-splitting was first introduced in [107] for a two users single-input single-output BC scenario. In [14], [108], RSMA was proposed as a powerful and generalized MA technique for RF systems. It was demonstrated that RSMA could potentially offer tactile improvements as a MA technique, by allowing wireless networks to efficiently serve multiple users with different capabilities in overloaded and underloaded scenarios. According to the key principle of RSMA, which relies on the implementation of linear precoding at the transmitter and SIC at the receiver, it has been shown that this MA scheme is capable of bridging the gap between NOMA and SDMA techniques. In RSMA, users' messages are split into common and private parts at the transmitter. Then, a combiner is used to multiplex the common parts of all users and encode them into a single common stream. Meanwhile, the private parts are encoded separately into multiple private streams. Subsequently, a linear precoder is used to mitigate MUI. Finally, all precoded streams are superimposed on the same signal and sent over a VLC BC channel. At each user, the common stream is decoded and the user's intended data is extracted. Then, interference introduced by the common

stream is eliminated using SIC, as in NOMA. Subsequently, the private part of each user message can be decoded, while treating the private parts of other users messages as noise, as in SDMA. This mechanism is illustrated in (Fig. 1, [14]).

RSMA depends mainly on the splitting design of messages and power allocation strategies between common and private parts of users' messages. Extensive research efforts have been devoted to the investigation of these issues in order to improve the efficiency of RSMA in the context of RF. In [14], the authors provided an analytical framework to study the performance of RSMA in MU-MISO BC channels. The reported results proved that RSMA outperforms NOMA and SDMA in terms of sum rate for different users' setups. Dai *et al.* investigated in [109] RSMA with massive MIMO and imperfect CSIT. They proposed a hierarchical-rate-splitting (HRS) framework where two different types of common messages are defined, which can be decoded by either all users or by a subset of them. Then, the associated sum rate performance was investigated in order to adjust the precoders of common messages. Numerical results illustrated the superiority of HRS compared to conventional techniques such as TDMA and BC with user scheduling. This work was extended in [110] to a MU millimeter wave (mmWave) case, where CSIT is either statistical or quantized. Similar to [109], Joudeh *et al.* proposed in [111] a hybrid RSMA messages precoding in order to achieve max-min fairness amongst multiple co-channel multicast groups. The superiority of their approach is proved through degree-of-freedom analysis and simulation results. The authors in [112] evaluated the robustness of RSMA, in the presence of hardware impairments, such as phase distortion and thermal noises, and the availability of perfect/imperfect CSIT. In addition, Abdelhamid *et al.* investigated in [113] the use of channel inversion precoding for MU-MIMO RSMA system, where phase-shift-keying was the adopted modulation scheme. Results showed that RS combined with channel inversion has a significant sum rate improvement compared to RS with ZF or other MA schemes. Moreover, the authors in [114] incorporated RS with DPC to achieve the largest rate region for MISO BC with partial CSIT for different network loads and users' deployments. In [115], Hao *et al.* proposed a practical scheme for private symbols encoding in RSMA using the conventional ZF beamforming. Then, they studied the sum rate performance for a two-user BC channel with limited CSI feedback. In [116], the authors considered the trade-off between the spectral efficiency and energy efficiency for RSMA in multi-antenna BC channels. It was shown that RSMA achieves a significant improvement in terms of spectral and energy efficiency. The use of RSMA in the downlink of a MISO SWIPT BC channel was investigated in [117]. The sum rate performance of rate-splitting was evaluated and compared with other MA schemes. A further study of RSMA in downlink CoMP JT networks was considered in [118], where results showed the superiority of RS in JT over SDMA- or NOMA-based JT. Also, in [119], Zhang *et al.* considered a cooperative rate splitting strategy based on the three-node relay channel, and demonstrated the enhanced performance of this scheme compared to cooperative-based NOMA. Similar results were reported in [120], where the max-min fairness

TABLE III  
VLC RELATED WORK ON SDMA.

Reference	System Model	Objective	Findings
[83], [84]	MU-MISO with BD precoding	Evaluation of the BER	With enough transmit power, a data rate of 100 Mbps is achieved for $BER=10^{-6}$
[85]	MU-MISO with ZF or ZF-DPC precoding	Maximization of the throughput and max-min fairness	ZF-DPC outperforms linear ZF, in particular when users are close to each other
[86]	MU-MISO with MMSE precoding	Evaluation of the optimal linear MMSE precoder under perfect and imperfect CSIT	Linear MMSE precoding is able to separate the broadcast signals at the VLC receivers
[87]	MU-MISO with MMSE/ZF precoding	Minimization of the MSE and evaluation of the BER	MMSE precoding achieves best results, while proposed simplified ZF approaches MMSE performance for a small number of (or dispersed) users
[88]	MU-MISO with ZF precoding	Maximization of the sum rate and max-min fairness	The generalized-inverse ZF design achieves better performance than the pseudo-inverse ZF design, in particular for high SNRs
[89]	MU-MISO with ZF precoding	Maximization of the sum rate	The proposed approach does not restrict the co-channel interference to zero, and thus, achieves a higher sum rate than conventional ZF techniques
[90]	MU-MISO with adaptive precoding	Derivation of closed-form expression and evaluation of BER under perfect and imperfect CSIT	Adaptive precoding provides significant performance enhancement compared to conventional channel inversion precoding
[91]	MU-MIMO OFDM with ZF/MMSE precoding	Evaluation of the spectral efficiency	Sub-carrier with higher index achieves a higher spectral efficiency, particularly for highly correlated users, and MMSE outperforms ZF for low transmit power and close users
[92]	MU-MISO with BD precoding	Maximization of the sum rate with imperfect CSIT	Robust precoding is designed using BD and WMMSE to suppress MUI and channel estimation errors
[93]	MU-MIMO with joint MMSE precoding and equalizing	Minimization of the MSE and evaluation of the BER in presence of CSIT errors	Proposed joint optimization method demonstrates BER improvements when experiencing imperfect CSIT
[94]	MU-STDMA	Minimization of the total scheduling time and power consumption	STDMA achieves full connectivity, and the proposed greedy algorithm significantly reduces the processing time
[95], [96]	Multi-cell MU-MIMO CoMP with MMSE precoding	Minimization of the WSMSE	Proposed approach realizes low-complexity interference mitigation compared to CoMP JT
[97], [98]	CoMP SDMA with ZF precoding	Evaluation of the Jain's fairness index and of area spectral efficiency	The proposed grouping algorithm achieves better area spectral efficiency-fairness trade-off compared to existing benchmarks
[99]	Multi-cell MU-MIMO joint MMSE precoding and equalizing	Minimization of the MSE and sum rate evaluation with imperfect CSIT	The joint design of the precoder and equalizer efficiently reduces inter-user interference and inter-cell interference, and achieves better performance compared to existing MMSE and max-rate designs
[100]	Multi-cell MU-MIMO CoMP with ZF precoding	Maximization of the sum rate	Partial cooperative precoding and coordinated precoding outperform per-cell coordinated precoding when the number of users is not large compared to the number of the LEDs or for high transmit power
[102], [103]	SDMA using ADTs	Evaluation of the throughput	The use of ADTs improves the performance of multi-user systems, and optical SDMA outperforms optical TDMA in terms of throughput
[104]	Attocell SDMA downlink using ADT	Derivation of closed-form expression for the spectral efficiency	inter-cell interference is mitigated and optical SDMA outperforms optical TDMA
[106]	MU-MIMO using ADTs	Maximization of the minimum SINR and evaluation of the rate per-user with imperfect CSIT	The proposed precoding and receiver design is robust to channel estimation errors and achieves significant gains compared to non-robust receiver design

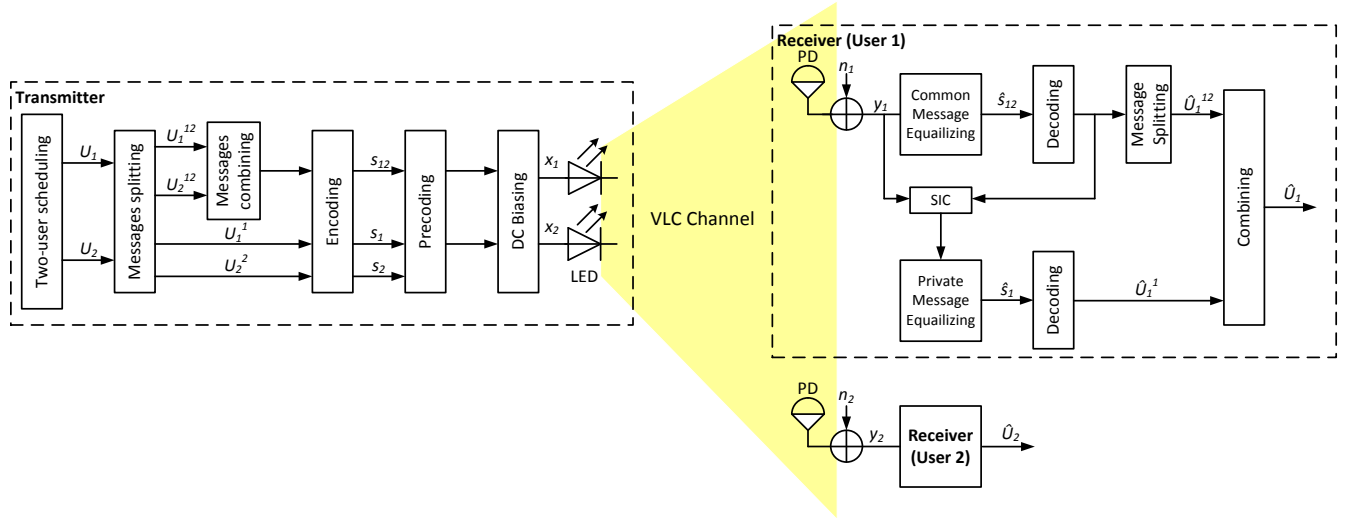


Fig. 6. RSMA-based two-user MISO VLC system.

was used as a metric for a  $K$ -user MISO BC with user's relaying cooperative communication. The authors in [121] adopted an RS strategy to overcome the saturation occurred in multi-pair MIMO relay systems with imperfect CSIT. The use of RSMA in cloud radio access network was considered in [122]. Yu *et al.* proposed an enhanced RSMA technique that outperforms the original RSMA through careful grouping of common signals that are chosen using hierarchical clustering with inter-UEs dissimilarity metric, defined based on channel directions. Additionally, the superiority of RSMA over other MA schemes was investigated for satellite systems in [123], where users achieved max-min fairness for multi-beam satellite communications under CSIT uncertainty with minimum inter-beam interference. Finally, RSMA was considered in [124] for cellular-connected drones, where the authors investigated the energy efficiency of RSMA and NOMA schemes in a mmWave downlink transmission scenario.

Despite the extensive research efforts on RSMA for different systems in the RF domain, its applicability in VLC systems has not yet been explored. Therefore, in this article, we provide preliminary results on the performance of RSMA in VLC systems, and compare its capacity gain with respect to existing VLC MA techniques. Furthermore, we give insights into the challenges and future research directions for RSMA-based VLC systems.

### B. RSMA-Based VLC

The concept of RSMA was proposed to a multi-antenna BC channel in [14] to bridge the gap between two extreme MA schemes, namely NOMA and SDMA. Mao *et al.* showed that RSMA works best in the multiple-input case. In the VLC context, this can be realized using several transmitting LEDs to create a BC channel towards several users. Hence, in this survey, we analyze the performance of RSMA in a downlink MU-MISO BC VLC system.

#### 1) System Model

For the sake of simplicity but without a loss of generality, we assume two transmitting LEDs that send messages to two single-PD users, as depicted in Fig. 6. Messages  $U_1$  and  $U_2$  are intended to users 1 and 2, respectively.  $U_1$  is divided into two parts: private part  $U_1^1$  and common part  $U_1^{12}$ . Similarly,  $U_2$  is divided into  $U_2^2$  and  $U_2^{12}$ . Then, the two private messages,  $U_1^1$  and  $U_2^2$ , are encoded into private streams  $s_1$  and  $s_2$ , respectively. Then, from a common codebook,  $U_1^{12}$  and  $U_2^{12}$  are combined and encoded into one common stream  $s_{12}$ . Without loss of generality, we assume that  $s_i$  ( $i \in \{1, 2, 12\}$ ) is randomly selected from a pulse amplitude modulation constellation with zero mean and normalized range  $\{-1, 1\}$ . Let  $\mathbf{s} = [s_1, s_2, s_{12}]^T$  be the transmitted symbols vector, with  $\mathbb{E}(\mathbf{s}\mathbf{s}^T) = \mathbf{I}$ . It is further assumed that the non-linear response of the LED is compensated through digital pre-disposition [125]. To reduce MUI, a linear precoding matrix  $\mathbf{P} = [\mathbf{p}_1, \mathbf{p}_2, \mathbf{p}_{12}]$  is considered, where  $\mathbf{p}_i = [p_{i,1} p_{i,2}]^T \in \mathbb{R}_{2 \times 1}$  is the precoding vector for the  $i^{\text{th}}$  stream. A DC bias  $\mathbf{d}_{DC} \in \mathbb{R}_{2 \times 1}$  is added in order to ensure positive signals, which is required by the LEDs. Hence, the transmitted signal,  $\mathbf{x} \in \mathbb{R}_{2 \times 1}^+$ , can be written as

$$\mathbf{x} = [x_1, x_2]^T = \mathbf{P}\mathbf{s} + \mathbf{d}_{DC} = \sum_{i \in \{1, 2, 12\}} \mathbf{p}_i s_i + \mathbf{d}_{DC} \quad (10)$$

and the received signal at the  $k^{\text{th}}$  PD, after optical-to-electrical conversion, is expressed as

$$y_k = \zeta(\mathbf{h}_k^T \mathbf{x} + n_k), \forall k \in \{1, 2\} \quad (11)$$

where  $\zeta$  is the conversion factor of any LED,  $\zeta$  is the responsivity of any PD,  $\mathbf{h}_k = [h_{k,1}, h_{k,2}]^T$  is the DC channel gain vector between the  $k^{\text{th}}$  PD and the transmitting LEDs, where each element is expressed as given in (9), and  $n_k \sim \mathcal{N}(0, \sigma_k^2)$  is the additive white Gaussian noise, representing the thermal and shot noise, with zero-mean and variance  $\sigma_k^2$ . Due to the

low mobility of indoor users, we assume that the channel gains are constant during the transmission, and that perfect CSI is available at the transmitter. In order to accurately design the precoding matrix  $\mathbf{P}$ , the following constraints need to be satisfied to ensure that the LEDs work in their dynamic range

$$\begin{aligned} L_1(\mathbf{p}_l) &= \sum_{i \in \{1,2,12\}} |p_{l,i}| \\ &= \min(d_{DC}, P_{\max} - d_{DC}), \forall l \in \{1, 2\}. \end{aligned} \quad (12)$$

The MMSE equalizer for the common stream is utilized at the  $k^{\text{th}}$  user for signal detection [86], followed by SIC as follows: First, user  $k$  decodes the common signal  $s_{12}$  while treating the other signals as noise. Hence, the received SINR at the  $k^{\text{th}}$  user, for the common signal, is expressed as

$$\gamma_k^{12} = \frac{(\mathbf{h}_k^T \mathbf{p}_{12})^2}{(\mathbf{h}_k^T \mathbf{p}_1)^2 + (\mathbf{h}_k^T \mathbf{p}_2)^2 + \hat{\sigma}_k^2}, \forall k \in \{1, 2\} \quad (13)$$

where  $\hat{\sigma}_k^2 = \sigma_k^2 / (\zeta\zeta)^2$  is the normalized received noise power. For the sake of simplicity, we assume that  $\zeta\zeta = 1$ , and thus  $\hat{\sigma}_k^2 = \sigma_k^2$ . Then, the effect of the common signal is removed using SIC. This allows for the detection of the private signal by first employing the MMSE equalizer, and then user  $k$  attempts to decode its private message  $s_k$ , while treating the signals of other user as noise. Consequently, the received SINR at user  $k$ , for its private signal, can be written as

$$\gamma_k^k = \frac{(\mathbf{h}_k^T \mathbf{p}_k)^2}{(\mathbf{h}_k^T \mathbf{p}_{\bar{k}})^2 + \sigma_k^2}, \forall (k, \bar{k}) \in \{(1, 2), (2, 1)\} \quad (14)$$

and the achieved data rate at user  $k$  is expressed by [14]

$$R_k^{12} = \log_2(1 + \gamma_k^{12}), \quad (15)$$

and

$$R_k^k = \log_2(1 + \gamma_k^k), \forall k \in \{1, 2\} \quad (16)$$

where  $R_k^{12}$  and  $R_k^k$  are the data rates for the common and private signals, respectively. In order to ensure successful decoding of the common stream  $s_{12}$  at both users, the common rate shall not exceed  $R_{12} = \min(R_1^{12}, R_2^{12})$ . The targeted common rate for each user can be achieved if  $R_{12}$  is adequately shared between the two users, i.e.,  $R_{12} = \sum_{k=1}^2 R_{k,\text{com}}$ , where  $R_{k,\text{com}}$  is the  $k^{\text{th}}$  user portion of the common rate. Consequently, the total achievable data rate of user  $k$ , denoted  $R_{k,\text{ov}}$ , can be expressed by [14]

$$R_{k,\text{ov}} = R_{k,\text{com}} + R_k^k, \forall k \in \{1, 2\}. \quad (17)$$

## 2) Problem Formulation

Although conventional precoders, such as ZF and ZF-DPC, are simple and can efficiently remove MUI, they suffer from performance degradation at low SNR values. Consequently, there is a need for optimal precoding in order to maximize an objective function, e.g., sum rate, weighted sum rate (WSR), proportional fairness, or max-min fairness [88], under QoS requirements and per-LED transmit power constraints to take into account the nature of the optical signals, which are real and positive valued. Inspired by the MMSE precoding method

## Algorithm 1 Alternating Optimization Algorithm

---

```

1: Initialize  $k \leftarrow 0, \mathbf{P}[k], R[k]$ 
2: repeat
3:    $k \leftarrow k + 1; \mathbf{P}[k-1] \leftarrow \mathbf{P}$ 
4:   Update the WMMSE weights  $\mathbf{w} \leftarrow \mathbf{w}(\mathbf{P}[k-1])$ 
5:   Update the receive filter gains  $\alpha \leftarrow \alpha(\mathbf{P}[k-1])$ 
6:   Solve (P1) using WMMSE transformation for updated  $(\mathbf{w}, \alpha)$ ,
   then update  $(\mathbf{P}, \mathbf{v})$ 
7: until  $|R[k] - R[k-1]| \leq \delta$ .

```

---

presented in [126], we maximize the WSR of the studied MU-MISO VLC system. For a given weights vector  $\mathbf{w} = [w_1, w_2]$ , the WSR maximization problem (P1) can be expressed as follows:

$$\max_{\mathbf{P}, \mathbf{R}_{\text{com}}} R(\mathbf{w}) = \sum_{k=1}^2 w_k R_{k,\text{ov}} \quad (\text{P1})$$

$$\text{s.t. } L_1(\mathbf{p}_l) \leq \varepsilon, \forall l \in \{1, 2\} \quad (\text{P1.a})$$

$$\sum_{k=1}^2 R_{k,\text{com}} \leq R_{12} \quad (\text{P1.b})$$

$$\mathbf{R}_{\text{com}} \geq \mathbf{0} \quad (\text{P1.d})$$

where  $\mathbf{R}_{\text{com}} = [R_{1,\text{com}}, R_{2,\text{com}}]$  is the common rate vector. (P1) is non-convex due to the presence of variables  $\mathbf{p}_k$  ( $k \in \{1, 2\}$ ) in the denominator of the SINR expressions (13)-(14). Thus, its solution is not straightforward. Similar to [127], we opt for problem reformulation, where the objective becomes the minimization of the weighted MMSE, and is achieved by jointly optimizing the WMMSE precoding vectors and MSE equalizer weights. To obtain a local optimum, we utilize alternating optimization (AO) detailed in Algorithm 1 [127], where  $k$  is the iteration index,  $\mathbf{w}$  is the MMSE weights vector,  $\alpha$  is the MSE receiver weights vector,  $\mathbf{v}$  is the transformation of  $\mathbf{R}_{\text{com}}$ , and  $\delta$  is the tolerance threshold. In order to converge to a maximum WSR, the algorithm alternates between WMMSE precoding design and MSE equalizer weights design. For further details on the AO procedure, we refer the reader to Sections IV and V in [127]. Finally, the reformulated problem can be solved using optimization software such as CVX in MATLAB [128]. It is noted that the AO algorithm converges faster and achieves better performance than other types of precoding optimization algorithms. However, its complexity increases with the number of users.

### 3) NOMA and SDMA as Special Cases of RSMA

As we mentioned earlier, RSMA is a generalized MA scheme, where NOMA and SDMA are special cases. To implement SDMA from RSMA, the common stream is allocated null power, and each user's message is encoded into a private stream only. Hence, the transmitted signal in this case is

$$\mathbf{x} = \mathbf{P}\mathbf{s} + \mathbf{d}_{DC} = \sum_{i \in \{1,2\}} \mathbf{p}_i s_i + \mathbf{d}_{DC} \quad (19)$$

and the received SINR at each user simplifies into (14).

Similarly, NOMA can be obtained from RSMA by encoding one of the users' messages as a private stream, i.e., the user with the strongest channel, and the signal of the second user is encoded into a common stream. Assuming that user 1 has

TABLE IV  
SIMULATION PARAMETERS.

Parameter	Symbol	Value
Number of LEDs per fixture	$Q$	3600 (60 × 60)
LED beam angle	$\varphi_{1/2}$	60°
PD area	$A_k (k = 1, 2)$	1 cm <sup>2</sup>
Refractive index of PD	$n$	1.5
Gain of optical filter	$T_s(\phi_{k,i}) (k = 1, 2)$	1
FoV of PD	$\phi_c$	60°

the strongest channel gain, then the transmitted signal in this case can be written as

$$\mathbf{x} = \mathbf{P}\mathbf{s} + \mathbf{d}_{DC} = \sum_{i \in \{1,2\}} \mathbf{p}_i s_i + \mathbf{d}_{DC} \quad (20)$$

and the associated SINRs of the first and second users are given by

$$\gamma_1^1 = \frac{(\mathbf{h}_1^T \mathbf{p}_1)^2}{\sigma_1^2} \quad (21)$$

and

$$\gamma_2^{12} = \min \left( \frac{(\mathbf{h}_1^T \mathbf{p}_{12})^2}{(\mathbf{h}_1^T \mathbf{p}_1)^2 + \sigma_1^2}, \frac{(\mathbf{h}_2^T \mathbf{p}_{12})^2}{(\mathbf{h}_2^T \mathbf{p}_1)^2 + \sigma_2^2} \right) \quad (22)$$

respectively. It is worth mentioning that the flexibility of RSMA comes at the expense of a slightly higher encoding complexity at the transmitter.

## VI. PERFORMANCE EVALUATION

We present in this section different scenarios for the application of RSMA in VLC systems, where we investigate their performance in terms of WSR, and then compare them to performances of SDMA and NOMA. Moreover, we study the impact of different users' locations within an indoor space.

We consider an RSMA-based MU-MISO VLC system, where two single-PD users are served by two or four LED fixtures in a room of size  $5 \times 5 \times 4 \text{ m}^3$ . The room configurations with the users' scenarios are detailed in Figs. 7–8, as follows. In both figures, main two users' location scenarios are considered. In the first (blue circles), users are located in the middle space of the room with a separation of 3 m, whereas in the second (green circles), users are located in the top of the room, with a smaller separation of 0.4 m. Between the two figures, the number and locations of LEDs is varied from 4 to 2. In addition, a third scenario is considered for the 4 LEDs case, where the separation between users is 0.94 m (yellow circle for user 1 and green circle of user 2). All coordinates are expressed in the 3D-space system. Furthermore, we assume the same optical devices characteristics as in [86], while the two users are allocated equal priority, i.e.,  $w_1 = w_2 = \frac{1}{2}$  in the objective function of (P1). Since the noise power is assumed unity, then the SNR designates the transmit power per-LED. The remaining parameters are detailed in Table IV.

Fig. 9 shows the WSR performance for RSMA, NOMA and SDMA, in "Scenario 1, 4 LEDs". It can be seen that RSMA outperforms both NOMA and SDMA, particularly at high SNR. In addition, SDMA performs better than NOMA, since the number of transmitter LEDs is larger than the number of users, allowing efficient management of MUI. However,

SDMA performs worse than RSMA due to the difficult channels alignment between users, caused by the nature of the VLC channel. In Fig. 10, the same comparison is made for "Scenario 2, 4 LEDs". With a smaller separation between users, channels are more correlated, which is reflected by the corresponding achievable performance. For instance, using RSMA, WSR=13 bits/s/Hz (RSMA) is achieved at SNR=40 dB, compared to WSR=15.5 bits/s/Hz in Fig. 9. Nevertheless, the performance of RSMA still exceeds that of both NOMA and SDMA. For SNRs below 35 dB, NOMA outperforms SDMA. Indeed, NOMA is able to distinguish different users using precoding and SIC receivers. However, for SNRs above 35 dB, this procedure is less effective, and direct beamforming using SDMA becomes privileged. Consequently, NOMA is favored at lower SNRs for low users separation, whilst SDMA is more performant for high SNRs. To examine the impact of the users separation, i.e., correlation between users channels, in Fig. 11, the WSR performance has been investigated for "Scenario 3" ( $U_1$  yellow +  $U_2$  green in Fig. 7), where the users separation is 0.94 m. It can be seen that the WSR performance of NOMA is improved compared to "Scenario 2." This is due to the reduced channel correlation between the two users, since the separating distance between users increased from 0.4 m to 0.94 m. Furthermore, SDMA and RSMA demonstrate improved performances, compared to "Scenario 2," due to the lower interference between users.

In Figs. 12-13, we consider the same scenarios, but with 2 LEDs. Similar to the previous results, the superiority of RSMA in terms of WSR over the other techniques is clearly illustrated. SDMA's performance is slightly degraded due to the smaller number of LEDs. Similar to Fig. 10, in Fig. 13 the SDMA performance is degraded at SNRs below 36 dB compared to NOMA, but outperforms the latter as the SNR increases. Finally, Fig. 14 illustrates the users' locations impact on the WSR performance of the RSMA scheme. We consider the room setup of 2 LEDs, and two users initially located in the middle of the room. From there, the first and second users travel to the east and west walls at the same constant speed, respectively. Thus, their physical separation increases until reaching its maximum 5 m (i.e., users have reached the opposite walls). It can be seen that WSR varies with the separation, until a maximum value is achieved for a separation equal to 3.6 m. This corresponds to users locations [-1.8, 0, 0.8] and [1.8, 0, 0.8], where the correlation between channels is low, but users are very close to one of the serving LEDs to capture maximal power. However, as this separation increases above 3.6 m, the WSR degrades due to longer distances between users and LEDs. It can be seen that these optimal users' locations are the same for different SNRs. Consequently, designing indoor spaces using RSMA-VLC requires a careful consideration of the LEDs' and users' locations.

## VII. OPEN ISSUES AND RESEARCH DIRECTIONS

In this paper, we reviewed different multiple access techniques proposed to improve the spectral efficiency of VLC systems and minimize the encountered VLC-specific interference issues. Then, we addressed a preliminary work on

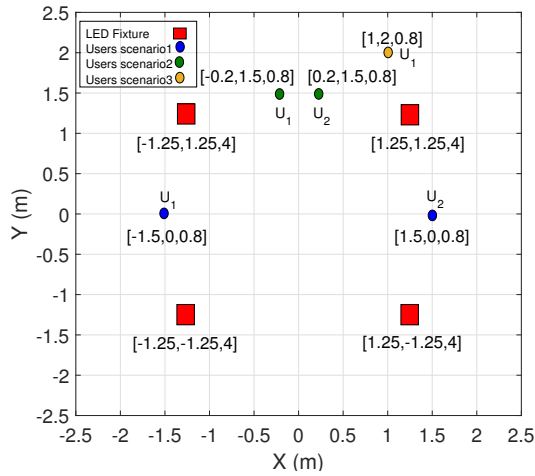


Fig. 7. Room configuration and users' scenarios (4 LEDs).

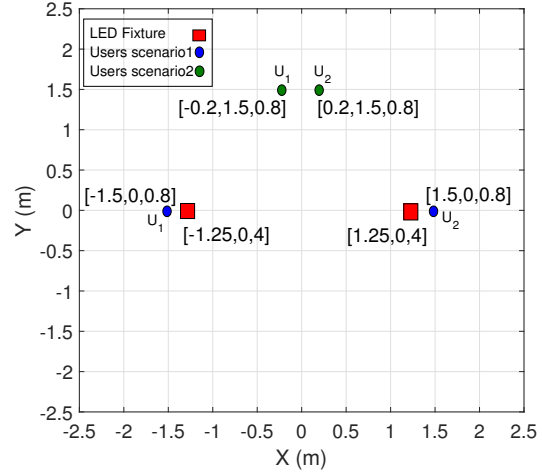


Fig. 8. Room configuration and users' scenarios (2 LEDs).

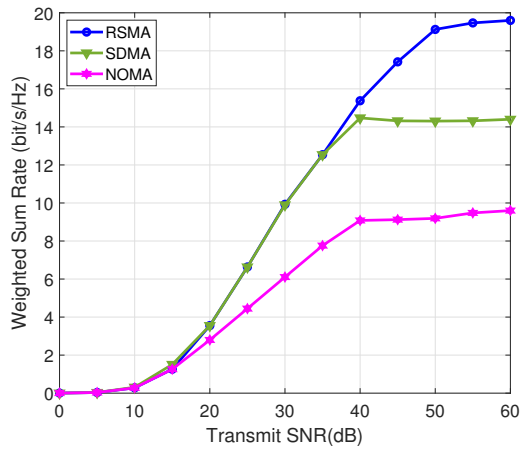


Fig. 9. WSR vs. SNR per LED array (Scenario 1, 4 LEDs).

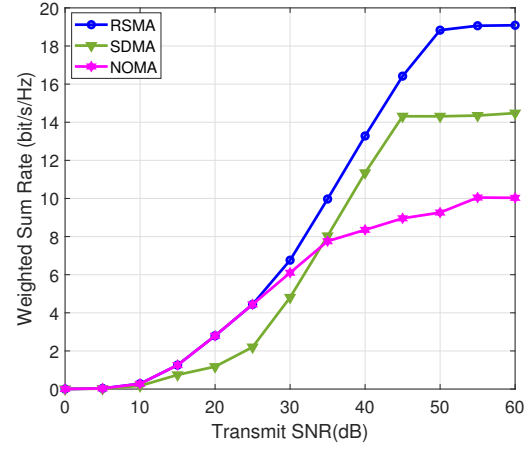


Fig. 10. WSR vs. SNR per LED array (Scenario 2, 4 LEDs).

the utilization of RSMA within VLC systems. It has been shown that RSMA is a powerful MA scheme that can provide high data rates and reliable VLC communications. However, several associated issues need to be addressed and analyzed for the practical realization of RSMA-VLC. For instance, the impact of the non-linear distortion caused by the different circuits components, such as LEDs, PDs, and analog/digital and digital/analog converters has to be investigated. Moreover, as a novel MA technique, more efforts are required to study the design of the physical and MAC layers. Hence, different performance metrics, modulation and coding schemes, and security issues, are open research problems in the RSMA-VLC. Additionally, optimal precoding and power allocation for RSMA-VLC are still open for investigation, where new linear and non-linear techniques can be proposed and optimized. Moreover, the current literature has mainly focused on the Gaussian noise assumption, but neglected the effect of ambient light, which can cause significant degradation in performance.

Other current assumptions include: the receiver is always

pointing upward, a LoS is always available and CSI is perfectly known. However, this may not be the case in practical scenarios, where the receiver can be differently oriented, the VLC link may experience shadowing and/or blockage, and CSI knowledge is imperfect. Consequently, the design and performance evaluation of RSMA-VLC systems that take into account these practical concerns have to be studied. Innovative solutions to circumvent the absence of a LoS may include enabling optical cooperative communications and device-to-device (D2D) communications. Indeed, optical cooperation among VLC transmitters guarantees reliable transmissions to users in a specific area [100], whereas in D2D communications, users with strong VLC links may help forwarding data to users with blocked VLC channels [129]. In the design of such systems, taking into consideration the different users' QoS may lead to improved performances.

Finally, the analysis of massive MIMO RSMA-VLC systems is another interesting open research problem.

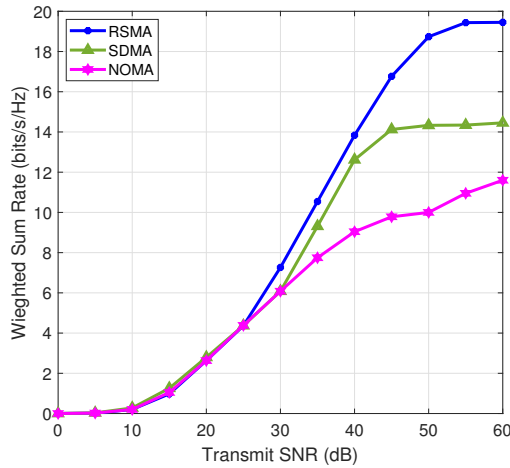


Fig. 11. WSR vs. SNR per LED array (Scenario 3, 4 LEDs).

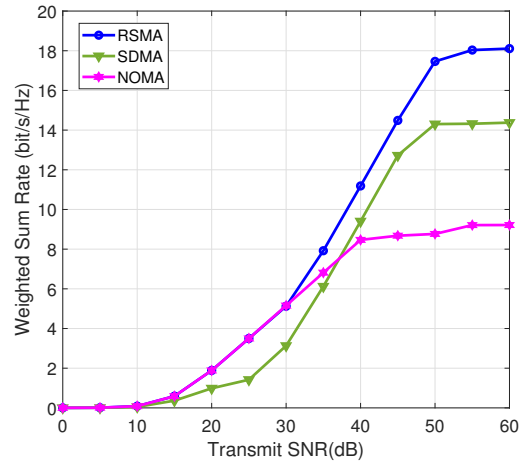


Fig. 13. WSR vs. SNR per LED array (Scenario 2, 2 LEDs).

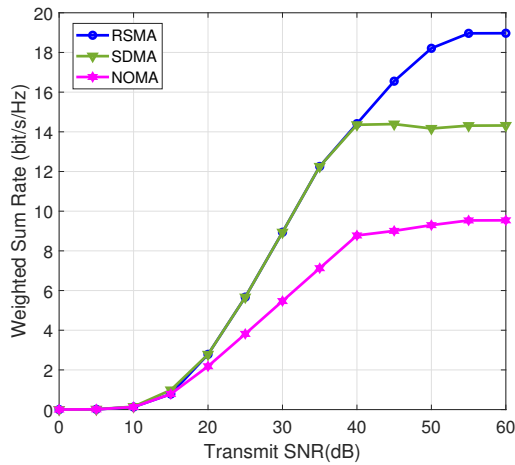


Fig. 12. WSR vs. SNR per LED array (Scenario 1, 2 LEDs).

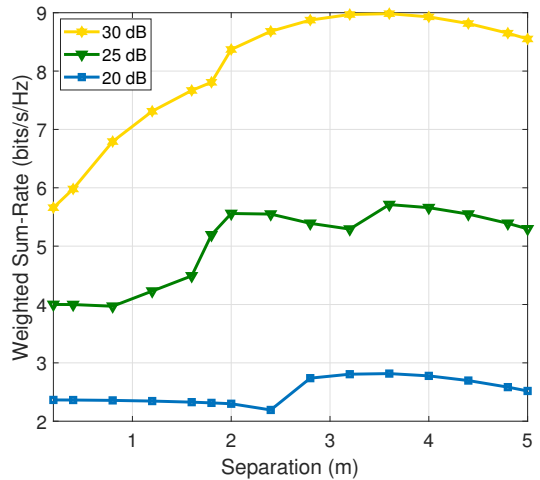


Fig. 14. Performance of RSMA for different users' locations/separations and SNRs.

### VIII. CONCLUSION

In this paper, we provided a conceptual background of several MA schemes for MIMO-VLC systems, along with their advantages and limitations. Specifically, our review covered NOMA and SDMA integration into VLC systems, showing how they minimize VLC interference and improve communications' performance. We reviewed also RSMA for RF systems, presented as a generalizing multiple access of NOMA and SDMA. Subsequently, we presented a preliminary study for the integration of RSMA into VLC systems, taking into consideration the per-LED power constraints. The SINR and WSR expressions are obtained for a two-user MISO VLC system, and results showed the flexibility of RSMA in generalizing NOMA and SDMA, at slightly increased design complexity. Through simulations, it has been proven that RSMA-VLC outperforms both techniques in terms of WSR. Also, RSMA is robust against channel correlation, and hence, it can be seen as a strong MA candidate for VLC in networks beyond 5G. Finally, a number of open issues and research directions, linked to MIMO RSMA-VLC, have been presented

and discussed.

### REFERENCES

- [1] T. Komine and M. Nakagawa, "Fundamental analysis for visible-light communication system using LED lights," *IEEE Trans. Consum. Electron.*, vol. 50, no. 1, pp. 100–107, Feb. 2004.
- [2] H. Elgala, R. Mesleh, and H. Haas, "Indoor optical wireless communication: Potential and state-of-the-art," *IEEE Commun. Mag.*, vol. 49, no. 9, pp. 56–62, Sep. 2011.
- [3] Z. Ghassemlooy, W. Popoola, and S. Rajbhandari, *Optical Wireless Communications: System and Channel Modelling with MATLAB*, 2nd ed. CRC Press, May 2019.
- [4] A. R. Ndjioungue, T. M. N. Ngatched, O. A. Dobre, and A. G. Armada, "VLC-based networking: Feasibility and challenges," *IEEE Network (Early Access)*, pp. 1–8, Jan. 2020.
- [5] L. Grobe, A. Paraskevopoulos, J. Hilt, D. Schulz, F. Lassak, F. Hartlieb, C. Kottke, V. Jungnickel, and K. Langer, "High-speed visible light communication systems," *IEEE Commun. Mag.*, vol. 51, no. 12, pp. 60–66, Dec. 2013.
- [6] D. Karunatilaka, F. Zafar, V. Kalavally, and R. Parthiban, "LED based indoor visible light communications: State of the art," *IEEE Commun. Surveys Tuts.*, vol. 17, no. 3, pp. 1649–1678, 3rd Quarter 2015.
- [7] F. Miramirkhani and M. Uysal, "Channel modeling and characterization for visible light communications," *IEEE Photon. J.*, vol. 7, no. 6, pp. 1–16, Dec. 2015.

- [8] IEEE, "IEEE draft standard for local and metropolitan area networks - Part 15.7: Short-range optical wireless communications," *IEEE P802.15.7/D3, August 2018*, pp. 1–412, Sep. 2018.
- [9] A. Jovicic, J. Li, and T. Richardson, "Visible light communication: Opportunities, challenges and the path to market," *IEEE Commun. Mag.*, vol. 51, no. 12, pp. 26–32, Dec. 2013.
- [10] P. H. Pathak, X. Feng, P. Hu, and P. Mohapatra, "Visible light communication, networking, and sensing: A survey, potential and challenges," *IEEE Commun. Surveys Tuts.*, vol. 17, no. 4, pp. 2047–2077, 4th Quarter 2015.
- [11] J. Armstrong, "OFDM for optical communications," *J. Lightw. Technol.*, vol. 27, no. 3, pp. 189–204, Feb. 2009.
- [12] J. A. Salehi, "Code division multiple-access techniques in optical fiber networks. I. Fundamental principles," *IEEE Trans. Commun.*, vol. 37, no. 8, pp. 824–833, Aug. 1989.
- [13] Z. Ding, Z. Yang, P. Fan, and H. V. Poor, "On the performance of non-orthogonal multiple access in 5G systems with randomly deployed users," *IEEE Signal Process. Lett.*, vol. 21, no. 12, pp. 1501–1505, Dec. 2014.
- [14] Y. Mao, B. Clerckx, and V. Li, "Rate-splitting multiple access for downlink communication systems: Bridging, generalizing, and outperforming SDMA and NOMA," *EURASIP J. Wireless Commun. and Network.*, no. 133, pp. 1–54, May 2018.
- [15] S. S. Bawazir, P. C. Sofotasios, S. Muhaidat, Y. Al-Hammadi, and G. K. Karagiannidis, "Multiple access for visible light communications: Research challenges and future trends," *IEEE Access*, vol. 6, pp. 26 167–26 174, May 2018.
- [16] M. Vaezi, G. A. Aruma Baduge, Y. Liu, A. Arafa, F. Fang, and Z. Ding, "Interplay between NOMA and other emerging technologies: A survey," *IEEE Trans. Cogn. Commun. Network.*, vol. 5, no. 4, pp. 900–919, 2019.
- [17] M. Obeed, A. M. Salhab, M. Alouini, and S. A. Zummo, "On optimizing vlc networks for downlink multi-user transmission: A survey," *IEEE Commun. Surveys Tuts.*, vol. 21, no. 3, pp. 2947–2976, 2019.
- [18] M. Sze and K. Ng, *Physics of Semiconductor Devices*. John Wiley and Sons Inc., 2007.
- [19] E. Monteiro and S. Hranilovic, "Design and implementation of color-shift keying for visible light communications," *J. Lightw. Technol.*, vol. 32, no. 10, pp. 2053–2060, May 2014.
- [20] L. Dai, B. Wang, Y. Yuan, S. Han, C. I, and Z. Wang, "Non-orthogonal multiple access for 5G: Solutions, challenges, opportunities, and future research trends," *IEEE Commun. Mag.*, vol. 53, no. 9, pp. 74–81, Sep. 2015.
- [21] H. Marshoud, V. M. Kapinas, G. K. Karagiannidis, and S. Muhaidat, "Non-orthogonal multiple access for visible light communications," *IEEE Photon. Technol. Lett.*, vol. 28, no. 1, pp. 51–54, Jan. 2016.
- [22] R. Mesleh, H. Elgala, and H. Haas, "On the performance of different OFDM based optical wireless communication systems," *IEEE/OSA J. of Optical Commun. and Network.*, vol. 3, no. 8, pp. 620–628, Aug. 2011.
- [23] E. Giacomidis, A. Tsokanos, C. Mouchos, G. Zardas, C. Alves, J. L. Wei, J. M. Tang, C. Gosset, Y. Jaouën, and I. Tomkos, "Extensive comparisons of optical fast-OFDM and conventional optical OFDM for local and access networks," *IEEE/OSA J. of Optical Commun. and Network.*, vol. 4, no. 10, pp. 724–733, Oct. 2012.
- [24] S. D. Dissanayake and J. Armstrong, "Comparison of ACO-OFDM, DCO-OFDM and ADO-OFDM in IM/DD Systems," *J. of Lightw. Technol.*, vol. 31, no. 7, pp. 1063–1072, Apr. 2013.
- [25] H. Elgala and T. D. C. Little, "Polar-based OFDM and SC-FDE links toward energy-efficient Gbps transmission under IM-DD optical system constraints [Invited]," *IEEE/OSA J. Opt. Commun. and Network.*, vol. 7, no. 2, pp. A277–A284, Feb. 2015.
- [26] S. Ali, E. Hossain, and D. I. Kim, "Non-orthogonal multiple access (NOMA) for downlink multiuser MIMO systems: User clustering, beamforming, and power allocation," *IEEE Access*, vol. 5, pp. 565–577, Jan. 2017.
- [27] F. Wei, W. Chen, Y. Wu, J. Li, and Y. Luo, "Toward 5G wireless interface technology: Enabling nonorthogonal multiple access in the sparse code domain," *IEEE Veh. Technol. Mag.*, vol. 13, no. 4, pp. 18–27, Dec. 2018.
- [28] S. M. R. Islam, N. Avazov, O. A. Dobre, and K. Kwak, "Power-domain non-orthogonal multiple access (NOMA) in 5G systems: Potentials and challenges," *IEEE Commun. Surveys Tuts.*, vol. 19, no. 2, pp. 721–742, 2nd quarter 2017.
- [29] M. H. Shoreh, A. Fallahpour, and J. A. Salehi, "Design concepts and performance analysis of multicarrier CDMA for indoor visible light communications," *IEEE/OSA J. of Opt. Commun. and Network.*, vol. 7, no. 6, pp. 554–562, Jun. 2015.
- [30] Y. Chen, Y. Chang, Y. Tseng, and W. Chen, "A framework for simultaneous message broadcasting using CDMA-based visible light communications," *IEEE Sensors J.*, vol. 15, no. 12, pp. 6819–6827, Dec. 2015.
- [31] J. Dai, K. Niu, and J. Lin, "Code-domain non-orthogonal multiple access for visible light communications," in *Proc. IEEE Globecom Wrkshps. (GC Wrkshps)*, Dec. 2018, pp. 1–6.
- [32] S. Lou, C. Gong, Q. Gao, and Z. Xu, "SCMA with low complexity symmetric codebook design for visible light communication," in *Proc. IEEE Int. Conf. Commun. (ICC)*, May 2018, pp. 1–6.
- [33] C. Rashidi, S. Aljunid, F. Ghani, H. A. Fadhil, and M. Anuar, "New design of flexible cross correlation (FCC) code for SAC-OCDMA system," *Procedia Eng.*, vol. 53, pp. 420 – 427, March 2013.
- [34] R. Razavi, R. Hoshyar, M. A. Imran, and Y. Wang, "Information theoretic analysis of lds scheme," *IEEE Communications Letters*, vol. 15, no. 8, pp. 798–800, 2011.
- [35] M. Al-Imari, M. A. Imran, R. Tafazolli, and D. Chen, "Subcarrier and power allocation for lds-ofdm system," in *2011 IEEE 73rd Vehicular Technology Conference (VTC Spring)*, 2011, pp. 1–5.
- [36] Y. Cai, Z. Qin, F. Cui, G. Y. Li, and J. A. McCann, "Modulation and multiple access for 5G networks," *IEEE Commun. Surv. Tuts.*, vol. 20, no. 1, pp. 629–646, 1st quarter 2018.
- [37] S. Tao, Y. Zuo, H. Yu, Q. Li, and Y. Tang, "Power allocation of non-orthogonal multiple access with variable on-off keying dimming control in visible light communication networks," in *Proc. IEEE Int. Conf. Commun. Tech. (ICCT)*, Nov. 2018, pp. 321–325.
- [38] Y. Cai, Z. Qin, F. Cui, G. Y. Li, and J. A. McCann, "Modulation and multiple access for 5g networks," *IEEE Communications Surveys Tutorials*, vol. 20, no. 1, pp. 629–646, 2018.
- [39] S. Al-Ahmadi, O. Maraqa, M. Uysal, and S. M. Sait, "Multi-User Visible Light Communications: State-of-the-Art and Future Directions," *IEEE Access*, vol. 6, pp. 70 555–70 571, Nov. 2018.
- [40] G. Pan, H. Lei, Z. Ding, and Q. Ni, "3-d hybrid vlc-rf indoor iot systems with light energy harvesting," *IEEE Transactions on Green Communications and Networking*, vol. 3, no. 3, pp. 853–865, 2019.
- [41] M. T. Alresheedi, A. T. Hussein, and J. M. H. Elmighani, "Uplink design in vlc systems with ir sources and beam steering," *IET Communications*, vol. 11, no. 3, pp. 311–317, 2017.
- [42] H. Marshoud, S. Muhaidat, P. C. Sofotasios, S. Hussain, M. A. Imran, and B. S. Sharif, "Optical non-orthogonal multiple access for visible light communication," *IEEE Wireless Commun.*, vol. 25, no. 2, pp. 82–88, Apr. 2018.
- [43] H. Marshoud, P. C. Sofotasios, S. Muhaidat, G. K. Karagiannidis, and B. S. Sharif, "On the performance of visible light communication systems with non-orthogonal multiple access," *IEEE Trans. Wireless Commun.*, vol. 16, no. 10, pp. 6350–6364, Oct. 2017.
- [44] C. Wang, Y. He, F. R. Yu, Q. Chen, and L. Tang, "Integration of Networking, Caching, and Computing in Wireless Systems: A Survey, Some Research Issues, and Challenges," *IEEE Commun. Surveys Tuts.*, vol. 20, no. 1, pp. 7–38, 1<sup>st</sup> quarter 2018.
- [45] T. Cover, "Broadcast channels," *IEEE Trans. Inf. Theory*, vol. 18, no. 1, pp. 2–14, Jan. 1972.
- [46] B. Lin, X. Tang, and Z. Ghassemlooy, "Optical power domain NOMA for visible light communications," *IEEE Wireless Commun. Lett.*, vol. 8, no. 4, pp. 1260–1263, Aug. 2019.
- [47] X. Liu, Z. Chen, Y. Wang, F. Zhou, Y. Luo, and R. Q. Hu, "BER analysis of NOMA-enabled visible light communication systems with different modulations," *IEEE Trans. Veh. Technol.*, vol. 68, no. 11, pp. 10 807–10 821, Nov. 2019.
- [48] R. C. Kizilirmak, C. R. Rowell, and M. Uysal, "Non-orthogonal multiple access (NOMA) for indoor visible light communications," in *Proc. 4th Int. Wrkshp. Optical Wireless Commun. (IWOW)*, Sep. 2015, pp. 98–101.
- [49] L. Yin, W. O. Popoola, X. Wu, and H. Haas, "Performance evaluation of non-orthogonal multiple access in visible light communication," *IEEE Trans. Commun.*, vol. 64, no. 12, pp. 5162–5175, Dec. 2016.
- [50] Z. Yang, W. Xu, and Y. Li, "Fair non-orthogonal multiple access for visible light communication downlinks," *IEEE Wireless Commun. Lett.*, vol. 6, no. 1, pp. 66–69, Feb. 2017.
- [51] H. Shen, Y. Wu, W. Xu, and C. Zhao, "Optimal power allocation for downlink two-user non-orthogonal multiple access in visible light communication," *J. Commun. and Info. Net.*, vol. 2, no. 4, pp. 57–64, Dec. 2017.



- [52] Y. Yapici and I. Guvenc, "NOMA for VLC downlink transmission with random receiver orientation," *IEEE Trans. Commun.*, vol. 67, no. 8, pp. 5558–5573, Aug. 2019.
- [53] W. Chu, J. Dang, Z. Zhang, and L. Wu, "Effect of clipping on the achievable rate of non-orthogonal multiple access with DCO-OFDM," in *Proc. 9th Int. Conf. Wireless Commun. Signal Process. (WCSP)*, Oct. 2017, pp. 1–6.
- [54] Y. Fu, Y. Hong, L. Chen, and C. W. Sung, "Enhanced power allocation for sum rate maximization in OFDM-NOMA VLC systems," *IEEE Photon. Technol. Lett.*, vol. 30, no. 13, pp. 1218–1221, Jul. 2018.
- [55] X. Guan, Q. Yang, and C. Chan, "Joint detection of visible light communication signals under non-orthogonal multiple access," *IEEE Photon. Technol. Lett.*, vol. 29, no. 4, pp. 377–380, Feb. 2017.
- [56] A. Wyner, "Recent results in the Shannon theory," *IEEE Trans. Inf. Theory*, vol. 20, no. 1, pp. 2–10, Jan. 1974.
- [57] V. Nguyen, H. D. Tuan, T. Q. Duong, H. V. Poor, and O. Shin, "Precoder design for signal superposition in MIMO-NOMA multicell networks," *IEEE J. Sel. Areas Commun.*, vol. 35, no. 12, pp. 2681–2695, Dec. 2017.
- [58] S. M. R. Islam, M. Zeng, O. A. Dobre, and K. Kwak, "Resource allocation for downlink NOMA systems: Key techniques and open issues," *IEEE Wireless Commun.*, vol. 25, no. 2, pp. 40–47, Apr. 2018.
- [59] M. Zeng, A. Yadav, O. A. Dobre, G. I. Tsiropoulos, and H. V. Poor, "Capacity comparison between MIMO-NOMA and MIMO-OMA with multiple users in a cluster," *IEEE J. Sel. Areas Commun.*, vol. 35, no. 10, pp. 2413–2424, Oct. 2017.
- [60] —, "On the sum rate of MIMO-NOMA and MIMO-OMA systems," *IEEE Wireless Commun. Lett.*, vol. 6, no. 4, pp. 534–537, Aug. 2017.
- [61] Z. Ding, F. Adachi, and H. V. Poor, "The application of MIMO to non-orthogonal multiple access," *IEEE Trans. Wireless Commun.*, vol. 15, no. 1, pp. 537–552, Jan. 2016.
- [62] Z. Ding, R. Schober, and H. V. Poor, "A general MIMO framework for NOMA downlink and uplink transmission based on signal alignment," *IEEE Trans. Wireless Commun.*, vol. 15, no. 6, pp. 4438–4454, Jun. 2016.
- [63] M. Morales-Céspedes, O. A. Dobre, and A. García-Armada, "Semi-blind interference aligned NOMA for downlink MU-MISO systems," *IEEE Trans. Commun.*, vol. 68, no. 3, pp. 1852–1865, Mar. 2020.
- [64] C. Chen, W. Zhong, H. Yang, and P. Du, "On the performance of MIMO-NOMA-based visible light communication systems," *IEEE Photon. Technol. Lett.*, vol. 30, no. 4, pp. 307–310, Feb. 2018.
- [65] X. Zhang, Q. Gao, C. Gong, and Z. Xu, "User grouping and power allocation for noma visible light communication multi-cell networks," *IEEE Commun. Lett.*, vol. 21, no. 4, pp. 777–780, Apr. 2017.
- [66] V. S. Rajput, D. R. Ashok, and A. Chockalingam, "Joint NOMA transmission in indoor multi-cell VLC networks," in *Proc. IEEE 30th Ann. Int. Symp. Personal, Indoor Mob. Radio Commun. (PIMRC)*, Sep. 2019, pp. 1–6.
- [67] J. Shi, J. He, K. Wu, and J. Ma, "Enhanced performance of asynchronous multi-cell VLC system using OQAM/OFDM-NOMA," *J. Lightw. Technol.*, vol. 37, no. 20, pp. 5212–5220, Oct. 2019.
- [68] A. Benjebbovu, A. Li, Y. Saito, Y. Kishiyama, A. Harada, and T. Nakamura, "System-level performance of downlink noma for future lte enhancements," in *2013 IEEE Globecom Workshops (GC Wkshps)*, 2013, pp. 66–70.
- [69] M. A. Sedaghat and R. R. Müller, "On user pairing in uplink noma," *IEEE Transactions on Wireless Communications*, vol. 17, no. 5, pp. 3474–3486, 2018.
- [70] Z. Q. Al-Abbasi and D. K. C. So, "User-pairing based non-orthogonal multiple access (noma) system," in *2016 IEEE 83rd Vehicular Technology Conference (VTC Spring)*, 2016, pp. 1–5.
- [71] L. Zhu, J. Zhang, Z. Xiao, X. Cao, and D. O. Wu, "Optimal user pairing for downlink non-orthogonal multiple access (noma)," *IEEE Wireless Communications Letters*, vol. 8, no. 2, pp. 328–331, 2019.
- [72] J. He, Z. Tang, and Z. Che, "Fast and efficient user pairing and power allocation algorithm for non-orthogonal multiple access in cellular networks," *IET Electronics Letters*, vol. 52, no. 25, pp. 2065–2067, 2016.
- [73] E. M. Almohimmah, M. T. Alresheedi, A. F. Abas, and J. Elmoghani, "A simple user grouping and pairing scheme for non-orthogonal multiple access in VLC system," in *Proc. Int. Conf. Transp. Opt. Nets. (ICTON)*, Jul. 2018, pp. 1–4.
- [74] Y. Yapici and I. Guvenc, "Non-orthogonal multiple access for mobile VLC networks with random receiver orientation," in *Proc. IEEE Glob. Commun. Conf. (GLOBECOM)*, Dec. 2019, pp. 1–6.
- [75] H. Abumarshoud, H. Alshaer, and H. Haas, "Dynamic multiple access configuration in intelligent LiFi atocellular access points," *IEEE Access*, vol. 7, pp. 62 126–62 141, May 2019.
- [76] M. B. Janjua, D. B. da Costa, and H. Arslan, "User pairing and power allocation strategies for 3d vlc-noma systems," *IEEE Wireless Communications Letters*, pp. 1–1, 2020.
- [77] V. K. Papanikolaou, P. D. Diamantoulakis, and G. K. Karagiannidis, "User grouping for hybrid vlc/rf networks with noma: A coalitional game approach," *IEEE Access*, vol. 7, pp. 103 299–103 309, 2019.
- [78] V. K. Papanikolaou, P. D. Diamantoulakis, Z. Ding, S. Muhaidat, and G. K. Karagiannidis, "Hybrid VLC/RF networks with non-orthogonal multiple access," in *Proc. IEEE Global Commun. Conf. (GLOBECOM)*, Dec. 2018, pp. 1–6.
- [79] X. Zhou, S. Li, H. Zhang, Y. Wen, Y. Han, and D. Yuan, "Cooperative NOMA based VLC/RF system with simultaneous wireless information and power transfer," in *IEEE/CIC International Conference on Communications in China (ICCC)*, Aug. 2018, pp. 100–105.
- [80] M. K. A. Aljohani, M. O. I. Musa, M. T. Alresheedi, and J. M. H. Elmoghani, "WDM NOMA VLC systems," in *Proc. 21st Int. Conf. Transport Opt. Nets. (ICTON)*, Jul. 2019, pp. 1–5.
- [81] Q. H. Spencer, C. B. Peel, A. L. Swindlehurst, and M. Haardt, "An introduction to the multi-user MIMO downlink," *IEEE Commun. Mag.*, vol. 42, no. 10, pp. 60–67, Oct. 2004.
- [82] Q. H. Spencer, A. L. Swindlehurst, and M. Haardt, "Zero-forcing methods for downlink spatial multiplexing in multiuser MIMO channels," *IEEE Trans. Signal Process.*, vol. 52, no. 2, pp. 461–471, Feb. 2004.
- [83] J. Chen, Y. Hong, Z. Wang, and C. Yu, "Precoded visible light communications," in *Proc. 9th Int. Conf. Inf., Commun. Signal Process.*, Dec. 2013, pp. 1–4.
- [84] Y. Hong, J. Chen, Z. Wang, and C. Yu, "Performance of a precoding MIMO system for decentralized multiuser indoor visible light communications," *IEEE Photon. J.*, vol. 5, no. 4, pp. 7 800 211–7 800 211, Aug. 2013.
- [85] Z. Yu, R. J. Baxley, and G. T. Zhou, "Multi-user MISO broadcasting for indoor visible light communication," in *Proc. IEEE Int. Conf. Acoustics, Speech and Signal Process.*, May 2013, pp. 4849–4853.
- [86] H. Ma, L. Lampe, and S. Hranilovic, "Robust MMSE linear precoding for visible light communication broadcasting systems," in *Proc. IEEE Globecom Workshops (GC Wkshps)*, Dec. 2013, pp. 1081–1086.
- [87] B. Li, J. Wang, R. Zhang, H. Shen, C. Zhao, and L. Hanzo, "Multiuser MISO transceiver design for indoor downlink visible light communication under per-LED optical power constraints," *IEEE Photon. J.*, vol. 7, no. 4, pp. 1–15, Aug. 2015.
- [88] T. V. Pham, H. Le-Minh, and A. T. Pham, "Multi-user visible light communication broadcast channels with zero-forcing precoding," *IEEE Trans. Commun.*, vol. 65, no. 6, pp. 2509–2521, Jun. 2017.
- [89] H. Shen, Y. Deng, W. Xu, and C. Zhao, "Rate maximization for downlink multiuser visible light communications," *IEEE Access*, vol. 4, pp. 6567–6573, Sep. 2016.
- [90] H. Marshoud, P. C. Sofotasios, S. Muhaidat, B. S. Sharif, and G. K. Karagiannidis, "Optical adaptive precoding for visible light communications," *IEEE Access*, vol. 6, pp. 22 121–22 130, Mar. 2018.
- [91] Q. Wang, Z. Wang, and L. Dai, "Multiuser MIMO-OFDM for visible light communications," *IEEE Photon. J.*, vol. 7, no. 6, pp. 1–11, Dec. 2015.
- [92] Z. Zeng and H. Du, "Robust precoding scheme for multi-user MIMO visible light communication system," in *Proc. 25th Europ. Signal Process. Conf. (EUSIPCO)*, Aug. 2017, pp. 2546–2550.
- [93] K. Ying, H. Qian, R. J. Baxley, and S. Yao, "Joint optimization of precoder and equalizer in MIMO VLC systems," *IEEE J. Sel. Areas Commun.*, vol. 33, no. 9, pp. 1949–1958, Sep. 2015.
- [94] P. Adasme, F. Seguel, I. Soto, and E. S. Juan, "Spatial time division multiple access for visible light communication networks," in *Proc. 1st South American Coll. Visible Light Commun. (SACVLC)*, Nov. 2017, pp. 1–6.
- [95] H. Ma, L. Lampe, and S. Hranilovic, "Coordinated broadcasting for multiuser indoor visible light communication systems," *IEEE Trans. Commun.*, vol. 63, no. 9, pp. 3313–3324, Sep. 2015.
- [96] H. Ma, A. Mostafa, L. Lampe, and S. Hranilovic, "Coordinated beamforming for downlink visible light communication networks," *IEEE Trans. Commun.*, vol. 66, no. 8, pp. 3571–3582, Aug. 2018.
- [97] L. Yin, X. Wu, and H. Haas, "SDMA grouping in coordinated multi-point VLC systems," in *Proc. IEEE Summer Topic Meet. Series (SUM)*, Jul. 2015, pp. 169–170.
- [98] L. Yin, X. Wu, H. Haas, and L. Hanzo, "Low-complexity SDMA user-grouping for the CoMP-VLC downlink," in *Proc. IEEE Global Commun. Conf. (GLOBECOM)*, Dec. 2015, pp. 1–6.

- [99] H. Yang, C. Chen, W. Zhong, and A. Alphones, "Joint precoder and equalizer design for multi-user multi-cell MIMO VLC systems," *IEEE Trans. Veh. Technol.*, vol. 67, no. 12, pp. 11 354–11 364, Dec. 2018.
- [100] T. V. Pham and A. T. Pham, "Coordination/cooperation strategies and optimal zero-forcing precoding design for multi-user multi-cell VLC networks," *IEEE Trans. Commun.*, vol. 67, no. 6, pp. 4240–4251, Jun. 2019.
- [101] J. B. Carruther and J. M. Kahn, "Angle diversity for nondirected wireless infrared communication," *IEEE Trans. Commun.*, vol. 48, no. 6, pp. 960–969, Jun. 2000.
- [102] S.-M. Kim and H.-J. Lee, "Visible light communication based on space-division multiple access optical beamforming," *Chin. Opt. Lett.*, vol. 12, no. 12, pp. 120 601–120 601, Dec. 2014.
- [103] Z. Chen and H. Haas, "Space division multiple access in visible light communications," in *Proc. IEEE Int. Conf. on Commun. (ICC)*, Jun. 2015, pp. 5115–5119.
- [104] Z. Chen, D. A. Basnayaka, and H. Haas, "Space division multiple access for optical attocell network using angle diversity transmitters," *J. Lightw. Technol.*, vol. 35, no. 11, pp. 2118–2131, Jun. 2017.
- [105] G. Xu and S. Li, "Throughput multiplication of wireless LANs for multimedia services: SDMA protocol design," in *Proc. IEEE Globecom Commun.*, vol. 3, Nov. 1994, pp. 1326–1332 vol.3.
- [106] H. Sifaou, A. Kammoun, K. Park, and M. Alouini, "Robust transceivers design for multi-stream multi-user MIMO visible light communication," *IEEE Access*, vol. 5, pp. 26 387–26 399, Nov. 2017.
- [107] Te Han and K. Kobayashi, "A new achievable rate region for the interference channel," *IEEE Trans. Inf. Theory*, vol. 27, no. 1, pp. 49–60, Jan. 1981.
- [108] B. Clerckx, H. Joudeh, C. Hao, M. Dai, and B. Rassouli, "Rate splitting for MIMO wireless networks: A promising PHY-layer strategy for LTE evolution," *IEEE Commun. Mag.*, vol. 54, no. 5, pp. 98–105, May 2016.
- [109] M. Dai, B. Clerckx, D. Gesbert, and G. Caire, "A rate splitting strategy for massive MIMO with imperfect CSIT," *IEEE Trans. Wireless Commun.*, vol. 15, no. 7, pp. 4611–4624, Jul. 2016.
- [110] M. Dai and B. Clerckx, "Multiuser millimeter wave beamforming strategies with quantized and statistical CSIT," *IEEE Trans. Wireless Commun.*, vol. 16, no. 11, pp. 7025–7038, Nov. 2017.
- [111] H. Joudeh and B. Clerckx, "Rate-splitting for max-min fair multigroup multicast beamforming in overloaded systems," *IEEE Trans. Wireless Commun.*, vol. 16, no. 11, pp. 7276–7289, Nov. 2017.
- [112] A. Papazafeiropoulos, B. Clerckx, and T. Ratnarajah, "Rate-splitting to mitigate residual transceiver hardware impairments in massive MIMO systems," *IEEE Trans. Veh. Technol.*, vol. 66, no. 9, pp. 8196–8211, Sep. 2017.
- [113] A. Salem, C. Masouros, and B. Clerckx, "Rate splitting with finite constellations: The benefits of interference exploitation vs suppression," 2019.
- [114] Y. Mao and B. Clerckx, "Beyond dirty paper coding for multi-antenna broadcast channel with partial CSIT: A rate-splitting approach," 2019.
- [115] C. Hao, Y. Wu, and B. Clerckx, "Rate Analysis of Two-Receiver MISO Broadcast Channel With Finite Rate Feedback: A Rate-Splitting Approach," *IEEE Trans. Commun.*, vol. 63, no. 9, pp. 3232–3246, Sep. 2015.
- [116] G. Zhou, Y. Mao, and B. Clerckx, "Rate-splitting multiple access for multi-antenna downlink communication systems: Spectral and energy efficiency tradeoff," 2020.
- [117] Y. Mao, B. Clerckx, and V. O. K. Li, "Rate-splitting for multi-user multi-antenna wireless information and power transfer," in *Proc. IEEE 20th Int. Wrkshp. Signal Process. Adv. Wireless Commun. (SPAWC)*, Jul. 2019, pp. 1–5.
- [118] —, "Rate-splitting multiple access for coordinated multi-point joint transmission," in *Proc. IEEE Int. Conf. Commun. Wrkshps. (ICC Workshops)*, May 2019, pp. 1–6.
- [119] J. Zhang, B. Clerckx, J. Ge, and Y. Mao, "Cooperative rate splitting for MISO broadcast channel with user relaying, and performance benefits over cooperative NOMA," *IEEE Signal Process. Lett.*, vol. 26, no. 11, pp. 1678–1682, Nov. 2019.
- [120] Y. Mao, B. Clerckx, J. Zhang, V. O. K. Li, and M. Arafah, "Max-min fairness of K-user cooperative rate-splitting in MISO broadcast channel with user relaying," 2019.
- [121] A. Papazafeiropoulos and T. Ratnarajah, "Rate-splitting robustness in multi-pair massive MIMO relay systems," *IEEE Trans. Wireless Commun.*, vol. 17, no. 8, pp. 5623–5636, Aug. 2018.
- [122] D. Yu, J. Kim, and S. Park, "An efficient rate-splitting multiple access scheme for the downlink of C-RAN systems," *IEEE Wireless Commun. Lett.*, vol. 8, no. 6, pp. 1555–1558, Dec. 2019.
- [123] L. Yin and B. Clerckx, "Rate-splitting multiple access for multibeam satellite communications," 2020.
- [124] A. Rahmati, Y. Yapici, N. Rupasinghe, I. Guvenc, H. Dai, and A. Bhuyan, "Energy efficiency of RSMA and NOMA in cellular-connected mmWave UAV networks," in *Proc. IEEE Int. Conf. Commun. Wrkshps. (ICC Wrkshps.)*, May 2019, pp. 1–6.
- [125] G. Stepniak, J. Siuzdak, and P. Zwiernicki, "Compensation of a VLC phosphorescent white LED nonlinearity by means of Volterra DFE," *IEEE Photon. Technol. Lett.*, vol. 25, no. 16, pp. 1597–1600, Aug. 2013.
- [126] D. H. Nguyen and T. Le-Ngoc, "MMSE precoding for multiuser MISO downlink transmission with non-homogeneous user SNR conditions," *EURASIP J. Advances in Signal Process.*, vol. 2014, no. 1, p. 85, Jun. 2014.
- [127] S. S. Christensen, R. Agarwal, E. De Carvalho, and J. M. Cioffi, "Weighted sum-rate maximization using weighted MMSE for MIMO-BC beamforming design," *IEEE Trans. Wireless Commun.*, vol. 7, no. 12, pp. 4792–4799, Dec. 2008.
- [128] M. Grant and B. SP, "CVX: MATLAB Software for Disciplined Convex Programming," <http://cvxr.com/cvx/>, Jan. 2014.
- [129] N. Raveendran, H. Zhang, D. Niyato, F. Yang, J. Song, and Z. Han, "VLC and D2D heterogeneous network optimization: A reinforcement learning approach based on equilibrium problems With equilibrium constraints," *IEEE Trans. Wireless Commun.*, vol. 18, no. 2, pp. 1115–1127, Feb. 2019.



**Shimaa Naser** received the M.Sc. degree in Electrical Engineering from the Jordan University of Science and Technology, Irbid, Jordan in 2015. Since 2018, she is pursuing her Ph.D. degree at the Department of Electrical and Computer Engineering of Khalifa University, Abu Dhabi, UAE. Her research interests include advanced digital signal processing techniques for visible light communications, MIMO techniques, orthogonal/non-orthogonal multiple access.



**Lina Bariah** (S'13-M'19) received the M.Sc. and Ph.D. degrees in communications engineering from Khalifa University, Abu Dhabi, United Arab Emirates, in 2015 and 2018. She is currently a Post-doctoral fellow with the KU Center for Cyber-Physical Systems, Khalifa University, UAE. She was a Visiting Researcher with the Department of Systems and Computer Engineering, Carleton University, ON, Canada, in summer 2019. Her research interests include advanced digital signal processing techniques for communications, channel estimation, cooperative communications, non-orthogonal multiple access, cognitive radios, and intelligent surfaces.



**Wael Jaafar** (S'08, M'14, SM'20) received the B.Eng. degree from the Higher School of Communication (SUPCOM), Tunis, Tunisia, in 2007, and the M.A.Sc. and Ph.D. degrees in Electrical Engineering from Polytechnique Montreal, QC, Canada, in 2009 and 2014, respectively. He was a Visiting Research Intern with the Department of Computer Science, UQAM, Montreal, Canada, between February 2007 and April 2007, and a Visiting Researcher within Keio University, Tokyo, Japan, between March 2013 and June 2013, and within Khalifa University, Abu

Dhabi, UAE, between November and December 2019. From 2014 to 2017, he has pursued a career in the telecommunications industry, where he has been involved in designing solutions for projects across Canada and abroad. In 2018, he held Research Fellow and Lecturer positions within the Computer Science Department of UQAM, Montreal, Canada. Since December 2018, Dr. Jaafar joined the Systems and Computer Engineering Department of Carleton University as an NSERC (National Sciences and Engineering Research Council of Canada) Postdoctoral Fellow. His current research interests include wireless communications, resource allocation, edge caching and computing and machine learning.



**Sami Muhaidat** (S'01-M'08-SM'11) received the Ph.D. degree in electrical and computer engineering from the University of Waterloo, Waterloo, ON, Canada, in 2006. From 2007 to 2008, he was an NSERC Post-Doctoral Fellow with the Department of Electrical and Computer Engineering, University of Toronto, ON, Canada. From 2008 to 2012, he was Assistant Professor with the School of Engineering Science, Simon Fraser University, Burnaby, BC, Canada. He is currently an Associate Professor with Khalifa University, Abu Dhabi, UAE, and a Visiting

Professor with the Department of Electrical and Computer Engineering, University of Western Ontario, London, ON, Canada. He is also a Visiting Reader with the Faculty of Engineering, University of Surrey, Guildford, U.K. Dr. Muhaidat currently serves as an Area Editor of the IEEE TRANSACTIONS ON COMMUNICATIONS, and he was previously a Senior Editor of the IEEE COMMUNICATIONS LETTERS and an Associate Editor of IEEE TRANSACTIONS ON COMMUNICATIONS, IEEE COMMUNICATIONS LETTERS and IEEE TRANSACTIONS ON VEHICULAR TECHNOLOGY. He was a recipient of several scholarships during his undergraduate and graduate studies and the winner of the 2006 NSERC PostDoctoral Fellowship Competition. Dr Muhaidat is a Senior Member IEEE.



**Paschalis C. Sofotasios** (S'07-M'12-SM'16) was born in Volos, Greece, in 1978. He received the M.Eng. degree from Newcastle University, U.K., in 2004, the M.Sc. degree from the University of Surrey, U.K., in 2006, and the Ph.D. degree from the University of Leeds, U.K., in 2011. He has held academic positions at the University of Leeds, U.K., University of California at Los Angeles, CA, USA, Tampere University of Technology, Finland, Aristotle University of Thessaloniki, Greece and Khalifa University of Science and Technology, UAE,

where he currently serves as Assistant Professor in the department of Electrical Engineering and Computer Science. His M.Sc. studies were funded by a scholarship from UK-EPSRC and his Doctoral studies were sponsored by UK-EPSRC and Pace plc. His research interests are in the broad areas of digital and optical wireless communications as well as in topics relating to special functions and statistics. Dr. Sofotasios serves as a regular reviewer for several international journals and has been a member of the technical program committee of numerous IEEE conferences. He currently serves as an Editor for the IEEE COMMUNICATIONS LETTERS and he received the Exemplary Reviewer Award from the IEEE COMMUNICATIONS LETTERS in 2012 and the IEEE TRANSACTIONS ON COMMUNICATIONS in 2015 and 2016. Dr. Sofotasios is a Senior Member IEEE and he received the Best Paper Award at ICUFN 2013.



**Mahmoud Al-Qutayri** (S'87, M'92, SM'02) is the Associate Dean for Graduate Studies – College of Engineering, and a Professor of Electrical and Computer Engineering at Khalifa University, UAE. He received the B.Eng., MSc and PhD degrees from Concordia University, Canada, University of Manchester, U.K., and the University of Bath, U.K., all in Electrical and Electronic Engineering in 1984, 1987, and 1992, respectively. Prior to joining Khalifa University, he was a Senior Lecturer at De Montfort University, UK. This was preceded by a Research

Officer appointment at University of Bath, UK. He has published numerous technical papers in peer reviewed international journals and conferences. He coauthored a book as well as a number of book chapters. His main fields of research include embedded systems design, applications and security, design and test of mixed-signal integrated circuits, wireless sensor networks, and cognitive wireless networks. During his academic career, Dr. Al-Qutayri made many significant contributions to both undergraduate as well as graduate education. His professional service includes membership of the steering, organizing and technical program committees of many international conferences.



**Octavia A. Dobre** (M'05–SM'07–F'20) received the Dipl. Ing. and Ph.D. degrees from Politehnica University of Bucharest (formerly Polytechnic Institute of Bucharest), Romania, in 1991 and 2000, respectively. Between 2002 and 2005, she was with New Jersey Institute of Technology, USA and Politehnica University of Bucharest. In 2005, she joined Memorial University, Canada, where she is currently a Professor and Research Chair. She was a Visiting Professor with Massachusetts Institute of Technology, USA and Universit'e de Bretagne

Occidentale, France. Her research interests include enabling technologies for beyond 5G, blind signal identification and parameter estimation techniques, as well as optical and underwater communications. She authored and co-authored over she refereed papers in these areas. Dr. Dobre serves as the Editor-in-Chief (EiC) of the IEEE Open Journal of the Communications Society and Editor of the IEEE Communications Surveys and Tutorials. She was the EiC of the IEEE Communications Letters, as well as Senior Editor, Editor, and Guest Editor for various prestigious journals and magazines. Dr. Dobre was the General Chair, Technical Program Co-Chair, Tutorial Co-Chair, and Technical CoChair of symposia at numerous conferences. shw|e was a Royal Society Scholar and a Fulbright Scholar. She obtained Best Paper Awards at various conferences, including IEEE ICC, IEEE Globecom and IEEE WCNC. Dr. Dobre is a Distinguished Lecturer of the IEEE Communications Society and a Fellow of the Engineering Institute of Canada.